Republic of Iraq
Ministry of Higher Education and Scientific Research
University of Baghdad
College of Education for Pure Science (Ibn-AL-Haitham)

Study the Lattice Strain and Particle Size of one Phase of Manganese Oxide by using Fourier Analysis of X-ray Diffraction

A Thesis
Submitted to the Council College of Education for Pure Science (Ibn-AL-Haitham)/ University of Baghdad in partial Fulfillment of the Requirements for the Degree of Master of Science
In Physics

By

Sarab Saadi Jahil

B.Sr c. 2000

Supervisor

Prof. Dr. Khalid Hellal Harbbi

2018 A.D *1439A.H*

بسم الله الرحمن الرحيم

(قَالُوا سُبْحَانَكَ لَا عِلْمَ لَنَا إِلَّا مَا عَلَّمْتَنَا ۖ إِنَّكَ أَنتَ الْعَلِيمُ الْحَكِيمُ)

صدق الله العظيم

سورة البقرة اية(٣٢)

Supervisor

I certify that this thesis titled "**Study the Lattice strain and particle size of one phase of Manganese oxide by using Fourier Analysis of x-ray diffraction**" was prepared by (Sarab Saadi Jheil), under my supervision at the Certification University of Baghdad \Education College for Pure Science (Ibn-AL-Haitham) / Department of Physics in partial fulfillment of the requirements for the degree of Master of Science in Physics.

Signature:

Name: Dr. Kaled Hellal Harbi.

Title: Professor.

University of Baghdad / College of Education for Pure Science (Ibn-AL-Haitham) / Department of Physics

Date 25/ 2/ 2018

The Council of the Department of Physics has approved the examining committee

Signature:

Name: Dr. Kareem A. Jasim

Titel: Professor.

University of Baghdad / College of Education for Pure Science (Ibn-AL-Haitham) / Department of Physics

Date: 25/2 / 2018

Certification of the discussion committee

We certify that we have read this Thesis , entitled ***"Study the Lattice strain and particle size of one phase of Manganese oxide by using Fourier Analysis of x-ray diffraction"*** and as examination committee, we examined the student (***Sarab Saadi Jheil***) on its contents , and that in our opinion it is a adequate for the partial fulfillment of requirements for the Degree of Master of Science in Physics .

Chairman:

Signature:

Name: Dr. Widad Hamdi Jasim

Title: Assistant Professor

Address: University of Baghdad

Date: 25 / 2 / 2018

Member:

Signature:

Name: Dr. Aseel Mustafa Abdul-Majeed

Title: Assistant Professor

Address: Mustansiriya University

Date: 8 / 2 / 2018

Member:

Signature:

Name: Dr. Raghad Subhi Abbas

Title: Assistant Professor

Address: University of Baghdad

Date: 25 / 2 / 2018

Supervisor:

Signature:

Name: Dr. Kaled Hellal Harbi

Title: Professor

Address: University of Baghdad

Date: 25 / 2 / 2018

Approved by the Council of the College for Pure Science Ibn-Al-Haitham /University of Baghdad:

Signature:

Name: Prof. Dr. Khalid Fahad Ali

Title: Professor

Dean of College

Date: 4 / 3 / 2018

Dedication

To the beacon of science, the master of creation to our Messenger Muhammad peace be upon him . . . . . .

To the spirit of my dear Father . . . . . .

To my Mother . . . . . .

To my children Zeid, Saif and Sama . . . . . .

To my Brothers and Sisters . . . . . .

Thanks and Appreciation

I thank God Almighty above all .....

I would like to express my thanks and appreciation to the Dr. Khaled Helal for his sincere efforts and I would like to thank the Dean of the College of Education for Pure Sciences (Ibn Al Haitham) . And to the President of the Department of Physics Professor Dr. Karim Ali Jassim to give them the opportunity to complete my studies And to all the professors of the respected physics department and to my colleagues in the respected physics department ..

Contents

List of Tables

List of Figures

List of Symbols

λ	The wavelength of the radiation
n	integer number
d_{hkl}	inter planer spacing

hkl	Miller indices
a	The lattice spacing
ε	The strain
2θ	Reflection angle
β_{hkl}	Full-width at half-maximum intensity
D	crystallite size
K	Scherrer constant
f(x)	the Fourier coefficient of g(x) and h(x)
g(x)	standard sample
h(x)	the integrated intensity profile function for the crystals
ω	Wavelength-distribution profile
θ	Bragg angle
F(t)	Fourier transforms
H(t)	Fourier transforms
G(t)	Fourier transforms
$F^{(\varepsilon)}$(L)	factor gives information about the micro strain of the lattice
$F^{(S)}$(L)	factor describes the contribution of crystallite size and stocking fault probability
$<\varepsilon^2>$	Mean-square strain

$D_{(hkl)}^{eff}$	Effective size
$\Delta(2\theta)$	The total angular range in 2θ scale
L	Fourier length
β_L	The integral breadth of the Lorentzian component
β_G	The integral breadth of the Gaussian component
TC	Texture Coefficient
I(h kl)	the measured relative intensity of a plane (h kl)
$I_\circ(hkl)$	the standard intensity of the plane taking from the JCPDS data
$I_\circ$	the ASTM standard intensity
Nr	the number of diffraction peaks and (hkl) are Miller indices
$< \varepsilon >$	Micro strains
ρ	The density of MnO 5.39 gm/cm3
δ	Dislocation density
SSA	Specific Surface Area
nm	nanometer
SA	part is Surface Area Angstrom
D*p*	the size (spherical shaped)
$< \varepsilon^2 >^{1/2}$	root – mean square strain

ε	strain
u	the strain energy density
σ	the stress
Y	Young's modulus
μ	Apparent Strain
Å	Angstrom

List of Abbreviations

MnO	Manganese mono oxide
XRD	X-Ray diffraction
LPA	Line profile analysis
FWHM	Full-width at half maximum intensity
FTIR	Fourier transform infrared transmission spectrometry
SEM	Scanning electron micrograph
W-H	Williamson–Hall
W-A	Warren - Averbach
nc	Nano crystalline
JCPDS	The Joint Committee on Powder Diffraction Standards
UDEDM	The Uniform Deformation Energy Density Model

USDM	The Uniform Stress Deformation Model
FT	Fourier transforms
SW	Scherrer Width
MCS	Mean Crystallite Size

Abstract

In this study, the Fourier method was used for the analysis of the x-ray diffraction pattern of Manganese Oxide for peaks (111), (200), (220), (311) and(222). The crystallite size of each x-ray peaks was calculated the Fourier method was also used to calculate the mean square lattice strain and the results were as follows, where the crystallite size equal to 7.64352 nm and the mean square lattice strain equal to 0.3566×10^{-4} . In order to determine the accuracy of the results of this method, other methods of analysis were used, such as the Debye - Scherrer method and Williamson–Hall method of analysis , and Modified Scherrer method for calculating the crystallite size. The Debye - Scherrer method was developed for computation strain and use in comparison. The value of crystallite size and strain of these four methods was compared with the value of crystallite size and mean square strain of the Fourier method. The Fourier method was developed to calculate other important variables in the crystalline structure, such a strain, which is equal to 7.4828×10^{-3} instead of the mean square strain and the density energy of the strain, which is equal to 2799614.7 dyne / cm^2 and the stress equal to 7.4828×10^8 dyne/cm^2. The results obtained from the Fourier method for calculating other parameters of the manganese oxide lattice for each peak of x-ray diffraction peaks such as the texture coefficient, its mean value equal to 0.99999 and the micro strains, which its mean value equal to 4.47×10^{-3} The dislocation density, its mean value are equal to 37.3×10^{15} (lines .m^2) and the specific surface area which Also its mean value is equal to 19,58432 $\times 10^4$ m^2/g of crystalline volume. A comparison was also made between the values of the square of strain and the apparent strain.

Chapter One
Introduction and Literature Review

1.1 Introduction

X-ray diffraction peak profile analysis is a powerful method for determining the microstructural properties of ultrafine-grained materials. The effects of crystallite size and lattice strain on peak broadening can be separated on the basis of their different diffraction order dependence. The standard methods of x-ray diffraction profile analysis based on the full width at half-maximum (FWHM), the integral breadths and on the Fourier coefficients of the profiles provide the apparent crystallite size and the mean-square of lattice strains [1].

X-ray micro-diffraction semblance using Fourier method at single crystal Alumina, Cu samples. The asymmetric and widened diffraction semblance recorded territory were analyzed by the Fourier analysis method . Average strain, particle size and dislocation density analysis [2].

There are two basic techniques of x-ray line profile analysis: Fourier space technique under which Fourier analysis (Warren 1968) also forms a part, and real space technique like ; integral breadth (Wagner and Aqua 1964); variance analysis (Wilson 1962) and peak- fitting methods (Keijseret *al* 1982). It has been shown that each of the above techniques leads to similar results for domain size and dislocation density [3].

Scherrer equation explains peak broadening in terms of incident ray divergence which makes it possible to satisfy the Bragg condition for non-adjacent diffraction planes. Once method effects have been excluded, the crystallite size is easily calculated as a function of peak width (full width at half maximum peak intensity (FWHM), peak position and wavelength. Warren and Averbach's way takes not only the peak width into account but also the shape of the peak. This method is based on a Fourier deconvolution of the measured peaks and the instrument broadening to obtain the true

diffraction profile. This process is capable yielding both the crystallite size distribution and lattice micro strain [4] .

In the case of sampled diffraction patterns, as in crystallography, Fourier refinement methods generally require a good approximation to the real solution before refinement is at all meaningful. The continuity of the observed Fourier transform partially removes this condition. One further piece of information, namely knowledge that the structure is of finite rather than infinite thickness, is sufficient to restrict the number of possible solutions to a very small number, and often to just one [5].

1.2 Literature Review

In (1994), the complex Fourier analysis method is used by L. L .Thompson and P. M. Pinsky to examine the dispersion and attenuation properties of the P- version Element method, the spectral system and the number of elements in the wavelength[6].

In (1999), S.G. Podorov *et al*, showed a new method of assessment based on Fourier analysis of x-ray diffraction data to determine the structural properties of super lattices. This technique is used for measurable x-ray reflection depending on non-complex analytical equations, distributions of strain and the integrate properties can be determined. The usefulness of this method can be obtained by analyzing the experimental data from an InxGa1-x As-Ga Assuper lattice on a GaAs sub state[7].

In (2000), P. Bala *et al*, reported that in this study, dry transition of calcium montormalonite was treated at variable temperatures between 30-50 °C. Methods of analysis of infrared and x-ray diffraction were used to describe thermal analysis. Microstructure standards and class perturbations such as crystal size and contrast between layers Calculate base reflection (001), using the Fourier method analysis and the method of variance, the

calculations revealed that the sample underwent a transition from a wet phase to a dehydrated phase at200°C. As a result, basal variation occurred as a result of temperature changes[8].

In (2001), B. Marinkovica *et al*, the world used a method of Warren-Averbach to find basic parameters and also to compare the microscopic parameters of the Warren-Averbach method with Balzar and Enzo methods, two other popular methods of size-strain analysis., using a powder of two nominal crystallite sizes, 80 Å and 200 Å. A 50%-50% and using a third sample consisting of a mixture of these substances This procedure provided good results and was much faster than the usual way[9].

In (2004), H. Chen , *et al*, used the x-ray micro-diffraction method for single crystal aluminum of (001) and (110) then analyzed the diffraction using Fourier technique. Then the of residual stress and strain explain in terms of dislocation cell structure. In plane crystal lattice rotation induced was measured by electron backscatter diffraction (EBSD) and compared with the FEM simulation [2] .

In (2005) , J .Amigó *et al*, reported that some scientists have studied quartz and the mullite corundum, where they have followed some integral range ways such as the Fourier analysis method Warren–Averbach way, the Williamson–Hall analysis Langford way. Particle sizes analyzed for mullite anisotropic in each set of samples. There are also small differences between two sets of samples. There is a relationship between microstructure statistics and chemical composition mineral composition of the sample and mechanical strength due to the composition of the studied porcelain in similar conditions[10].

In (2005), M.S. Haluska *et al*, reported that SiO_2 method was calculated in the form of atomic shells and was calculated using x-ray methods and Fourier method. The Warren - Averbach method showed samples that were repeated

several times. Distribute the primary particle size of the MgO over time as well as the new crystallization of the MgO for 60 minutes while the lattice strain decreased sharply before 60 minutes of solubility[11].

In (2008),A .Milev) *et al*, reported that the research into the development of the structure to nano crystalline graphite shaped from ball grinding in explored using the Fourier technique of expansion diffraction peak features matching with the double-Voigt method which analyzed out of the plane to the plane particle size ratios that the crystals became thinner and gradually thinned, the linearity the root means a square strain and the size of the reciprocating particles along the axis of the stack reveals the size of the border areas gradually degraded at the expense of the crystalline areas required[12].

In (2009), V.I. Monin *et al*, reported that in this paper computer simulation is used both to obtain the criterions of existence of surface stress gradients and to resolve the problem of experimental determination of stress gradients by x-ray diffraction technique. Fourier analysis, widely used in different fields of modern physics, can be applied to study the broadening of diffraction profile caused by the presence of surface stress gradient. The function responsible for diffraction line broadening depends on x-ray penetration into the analyzed material and the magnitude of stress gradient parameters. Extracting this function (distortion function) allows using it in the determination of stress distribution near the surface of a material [13].

In (2011), R. Sen *et al*, reported that the classical method of the Williamson- Hall was used in addition to Williamson -Hall modified method to calculate the particle size and results obtained from two methods when studying nano crystalline ceria nano powder material by a high-energy mill ball of plate formed as received by the Cierra nano powders, after comparing the results it was found that the method obtained from the modified

Williamson-Hall was lower than the particle size with the increase in grinding time which became better[14].

In (2015), T.Many *et al*, studied the manufacture of ZnO nanowires (NWs). Several techniques have been used, including the SEM, of the ZnO nano-particles and also using the Debye scherrer method of the same sample[15].

In (2016), Dr. Ziad *et al* , reported that in this study Magnesium oxide (MgO) nanoparticles are synthesized by Sol - Gel method using Mg(NO3)2.6H2O as a precursor and different molar concentrations of NaOH as a stabilizing agent. X-ray diffraction pattern (XRD) reveals single phase fcc structure with a lattice constant 4.21Å . Scanning electron microscopy (SEM) showed the aggregated irregular and tiny crystals of as prepared MgO nanoparticles. By using Williamson-Hall equation , the particle sizes vary within the range of 11.27 -14.44 nm. [16].

In (2017), Sh. Yadav *et al*, reported that in this research studied of x-ray diffraction (XRD) technique, which clearly indicates the presence of hexagonal Wurtzite structure for pure single doped and tri-doped ZnO-NPs. The effect of different dopant on crystallite sizes and lattice strain of ZnO-NPs were then studied using modified form of Williamson-Hall (W-H) method and Size-Strain plot method. We also calculated crystallite sizes of doped and pure ZnO NPs with the help of Debye-Scherrer method. The three form of W-H plot i.e. UDM, USDM and UDEDM and SSP model were then used to calculate parameters such as strain, stress and energy density for all the reflection peaks of XRD corresponding to ZnO lying in the range $2\theta = 15^{o}–80^{o}$ [17].

1.3 The Aim of The Work

The aim of this search is to use the Fourier method to analyze the profile lines broadening of x-ray diffraction to determine the lattice strain and particle size and to also determine the properties of crystal structure of manganese oxide. Then comparing the results of lattice strain and particle size with the results of other analysis methods to know the accuracy of the values calculated in the Fourier method as a method adopted in the research . As well as to develop this method for the purpose of calculating other important parameters of the lattice .

Chapter Two
The Theoretical Part

2.1 Introduction

This chapter contains a detailed explanation of x-ray diffraction method and how it can achieve Bragg`s law and explain the powder x-ray diffraction method to obtain the pattern of x-ray diffraction and the causes of broadening the side lines of the x-ray. Simple methods of analysis were also explained such as Scheerer modified method and Williamson–Hall method. The Fourier method was also presented as an accurate method of giving the results of the analysis. The equations used to calculate important parameters of crystalline structure, as well as strain and crystallite size, were presented. Due to the accuracy of the Fourier method, it has been developed through mathematical treatments for the value of emotion and thus obtained three models explained in detail in this chapter. However, the Sheareer method was also modified to calculate strain of lattice. This is another model added to the three models mentioned .

2.2 X-ray diffraction

Braggs and von Laue were the first to understand x-ray diffraction. Atomic electrons move by the oscillating electric field of the x-ray incident and their accelerations. The incident electrons react charged from the atom in the electron diffraction with substances penetrating them into relatively small distances reach up to a few hundred angstrom before they suffer from flexible or inflexible dispersion. In neutron diffraction pioneered by Shull, the incident neutron wave function interacts with nuclei or electron spins. These three diffraction procedures involve very dissimilar physical technique. The Brag law interprets x-ray diffraction, which determines the propagation angles where peaks and intensity are strong, and by determining the location and intensity of the diffraction peaks measuring the composition that is unique to a particular chemical compound. The crystalline planes will make the

diffraction, according to Bragg`s Law when an x-ray beam with a known wavelength is incident to a crystalline solid, the deflected waves will not be in phase except when the following relationship is satisfied:

n λ= 2d_{hkl} sinθ ……...……..…….(2.1)

Where

n: integer number

θ: Brags angle

λ: the length of the wave

d : inter planer spacing.

Eq.(2.1) is Bragg`s law, with this equation when we have constructive interface we can determine the distance between atomic planes and therefore we can determine the properties crystalline structure of material .

.

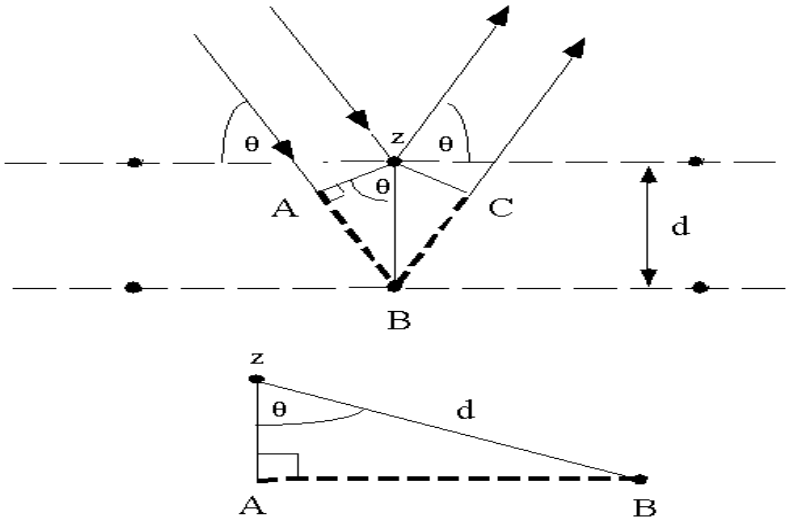

Figure 2.1: Schematic of diffraction to prove Brags law.

Figure (2.1) shows schematic of diffraction to substantiate Bragg's law, Through the following relationship can be used to obtain the lattice spacing of a particular cube system :

$$d = \frac{a}{\sqrt{h^2+k^2+l^2}} \quad \text{.....(2.2)}$$

Where (hkl) are the Miller indices of the Bragg plane and a is the lattice spacing of the cubic crystal, combining this relation with Bragg's law.

$$\left(\frac{\lambda}{a}\right)^2 = \left(\frac{(\sin\theta)^2}{h^2+k^2+l^2}\right) \text{.....(2.3)[18].}$$

Produce diffraction by a crystal of x-ray scattering though individual atoms in the crystal. The diffraction intensity dependent on scattering by all the atoms in the crystal. The scattering intensity is a function of the angle between the incident beam and scattering direction 2θ. Diffractometer functions are the x-ray diffraction detecting from material and the measuring of diffraction intensity. Figure(2.2) show the geometrical order of x-ray source sample and detector. The x-ray radiation generated through an x-ray tube passes of special slits. These solder slits are commonly used in the diffractometer. They are produce from asset of closely spaced thin metal plates parallel to plane to prevent beam divergence in the director perpendicular to the figure plane. A divergent x-ray beam crossing through the slits strikes the specimen [19]**.**

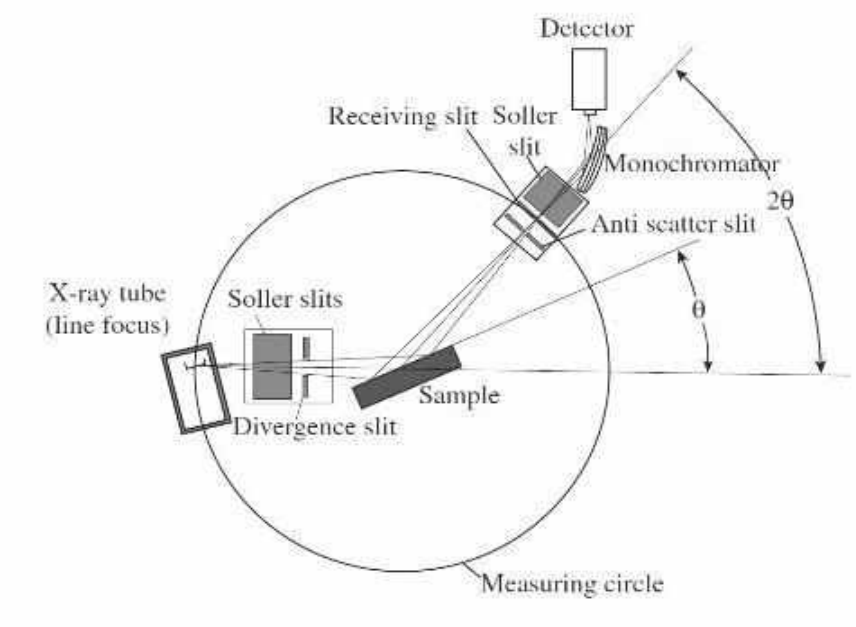

Figure 2.2: Geometric arrangement of x-ray diffractometer.

X-ray diffraction spectra can be distorted by any factor altering the lattice parameters of the crystalline specimens. The residual stress in the solid samples may also change the position of the peak of the diffraction in the spectrum. [20]. The strain can be measured empirical through measuring the peak Location 2θ, and Bragg equation for a value of d. If we know the unstrained inter-planar spacing d then, wide angle x-ray diffraction with conventional experimenter equipment can be applied as instrument .In this research was picked the micro strain and particle size of x- ray diffraction such as of MnO nano particles using Cu Kα as shown in figure (2.3) .

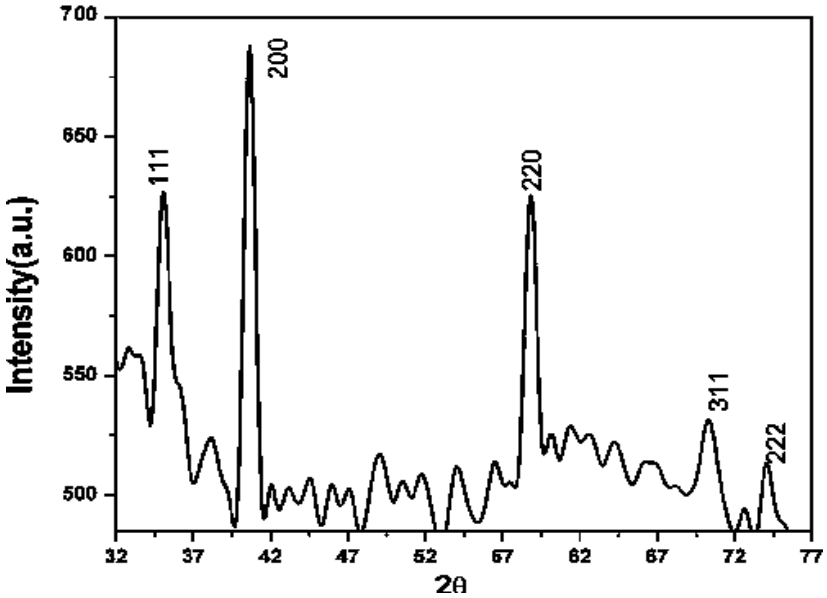

Figure (2.3) : XRD of MnO nanoparticles[21].

Form ASTM card 00-003-1145 (Fixed Slit Intensity) - Cu Kα1, 1.54056A manganese mono oxide with cubic system and face centered cubic lattice. The lattice fringes with spacing of (0.44 nm)are in good agreement with the lattice constant of (a = 0.444 nm) in MnO nanoparticles [22].

2.3 Powder X-ray Diffraction

X-ray powder diffraction (XRD) is a rapid analytical technique primarily used for phase identification of a crystalline material and can provide information on unit cell dimensions. The analyzed material is finely ground, homogenized, and average bulk composition is determined. X-ray diffraction is based on constructive interference of monochromatic x-rays and a crystalline sample. The interaction of the incident rays with the sample produces constructive interference and a diffracted ray when conditions satisfy Bragg's Law. These diffracted x-rays are then detected, processed and counted. By scanning the sample through a range of 2 θ angles, all possible diffraction directions of the lattice should be attained due to the random orientation of the powdered material. Conversion of the diffraction peaks to

d-spacing allows identification of the mineral because each mineral has a set of unique d-spacing. Typically, this is achieved by comparison of d-spacing with standard reference[23]. Many substances are not obtainable in a mono crystal style. furthermore, powders and bulk substances are more readily attackable procedural and minimal expensive. A powder diffraction testing demand an order of amount lower time than a mono crystal empirical, so powder diffraction is predominantly. However, because data are of minimum quality and peaks are mostly supremely overlapped at supremely diffracting angles. The powder diffraction was generally utilized for specific stage analysis. Through advances by Rietveld [24,25], utilize in structure analysis, seeming construction refinement .

2.4 Diffraction-Line Broadening

Radiation emission from surface of material planes can be define as θ that satisfy the equation of diffraction . In the theoretical aspect, high intensity from an polycrystalline should consist of diffraction peak without display at some are separate diffraction θ. However, the instrument and specimen broadening of the peak, and the observed peaks is a folds of three variables [26,27].

$$h(2\theta) = (\omega\theta * y)(2\theta) * f(2\theta) \quad (2.4)$$

the effect of instrument on the peak is :

$$g(2\theta) = (\omega\theta * y)(2\theta) \quad (2.5)$$

Where

ω: Wavelength-distribution profile

θ: Bragg angle

y: geometrical-aberration profile

f(2θ): Pure specimen (physically) broadened profile and its Fourier transform

h(2θ): observed broadened profile and its Fourier transform

g(2θ) :Instrumentally broadened profile and its Fourier transform

To obtain a sample nanostructure guide, the sample broadening peak must be extracted from the peak (h), the past of sample broadening in general, any lattice imperfection will cause also the diffraction peak width. Then the dislocations defect Schottky, Frankel and same defects it during the lattice distortion. If a crystal is fracture into smaller part diffracting by defect, then the grain size broadening happens.

2.5 Source of Line Broadening

The microscopic case on the material can also presentation covers the all of peak broadening means instrumental in the line, crystallite size width and distortion width . This two width are full width at mid intensity and not equal to breadth (β) it's means the width of a rectangle with the same area of the line. the Scherrer equation [28].

$D = K \lambda/\beta \cos \theta$ ……..(2.6)

Where

D : the Crystallite size

K : Scherrer constant and the value is taken to be K=(0.89),

λ : The wavelength of the radiation, λ cu kα1 = 0.15406

β : The breadth of the peak (in radians) located at 2θ

θ : The Bragg angle measured

the distortion broadening is determined by Stokes and Wilson [29,30].

$$\varepsilon = \frac{\beta}{4\tan\theta} \quad \text{……………………………………………(2.7)}$$

where

ε : the lattice strain.

β : the line broadening at half the maximum intensity (FWHM)

2.6 Fourier Analysis Method

The shape of the x-ray diffraction of a crystal can be determination in terms of scattering intensity as function of scattering direction defined by the scattering parameter, or by the scattering angle 2θ from equation(2.1). Empirically the value of h(2θ) for the sample, and the function f (2θ) can be calculate by the volume of h(2θ)and g(2θ)[31]. In addition to the line broadening due to the particle size and strain ,there is a source of broadening due to the equipment itself (slit size, penetration in the sample, imperfect focusing). The source of broadening is called instrumental broadening. A Modification for the contribution of the contributory broadening can be made considering that the experimental profile h(x) is a convolution of the sample profile f(x) and the instrumental contribution g(x) .

$$h(x) = f(x) \times g(x) \quad \text{……………………………………………(2.8)}$$

Demonstrated that F(x) could be obtained the Fourier coefficient of g(x) and h(x). The g(x) profile is obtained through the acquisition in the same conditions as the experimental profile h(x), of a standard sample. The observed x-ray diffraction lien profile, h(ε)is the convolution of the instrumental profile, g(ε) and pure diffraction profile f(ε)[32]. Simplified

integral-breadth technique that depends on some assumed analytical forms of the peak profiles. The iterative technique of consecutive folding's. Deconvolution technique of Stokes from equations (2.5) and (2.8), it follows that deconvolution can be performed easily in Fourier transforms of respective functions [33]:

$$F(t) = \frac{H(t)}{G(t)} \quad \text{.....(2.9)}$$

Where F(t),H(t) and G(t) are Fourier transforms used to calculate the crystallite size and lattice strain by use in also the equation (2.10) and (2.11).

$$\text{Function of size (F.S)} = e^{\frac{-L}{D}} \quad \text{.....(2.10)}$$

$$\text{Function ofstrain (F.}\varepsilon) = e^{-\frac{2\pi^2 <\varepsilon_L^2> h_\circ^2 L^2}{a^2}} \quad \text{.....(2.11)}$$

Where

D:the effective size

$< \varepsilon^2 >_{hkl}$: the micro strain of the lattice

$h_\circ^2 = h^2+k^2+l^2$

$c^2 = 2\pi^2 h_\circ^2/a^2$ [34].

X-ray diffraction from crystal planes happens at welled fined angles that satisfy Bragg equation(2.1). Numerically, intensity diffracted from an unlimited crystal should contain of diffraction lines without width at some discrete diffraction angles. However, both method and specimen broaden the diffraction lines, and the observed line profile is a convolution of three functions [35]. L is the Fourier length from equation.

$$L = \lambda /2 (\sin \theta_2 - \sin \theta_1) \quad \text{.....(2.12)}$$

Where the peak profile is calculated from θ_1 to θ_2 and λ is the x-rays' wavelength [36].

2.7 Deby- Scherrer Method

The Scherrer method that connects, crystallites or the size of sub-micrometer particles, in a solid to the broadening of a peak in a diffraction pattern. It is named after Paul Scherrer [37]. It is used in the determination of particles size in the form of powder as from equation (2.6) [38]. Through studies he concluded that the size of the crystals was less than 100 nm equation (2.6), nano crystallite size in x-ray diffraction to calculating FWHM. The target of modified scherrer equation of fired. This method show ln β to word ln $\frac{1}{cos\theta}$ and achieve the intercept of a smallest squares line reversion ln$\frac{K\lambda}{D}$ from which a sole value of D is acquired through all of the obtainable peaks[39]. If the crystals are small, the Prague tops are enlarged in a diffraction pattern that is inversely proportional to the size of the particles. Thus the expansion measurement gives a method for estimating the particle size by Debye –scherrer [40]. This method appears valid as it gives interpose values between Gaussian and consuming Lorentzian assumptions. Another solution, a little bit more time, is to construct a change table between the observed the pure profile SW(B) and $\beta(2\theta)$. This table may be found by convolution of the peak of a well crystallized mica powder, taken to be the instrumental profile, with a calculated pure profile assumed to be represented by a symmetrical Pearson-VII peak. We used this solution in one of the following examples. The Scherrer equation [41]:

$$\beta_{\Delta 2\theta(hkl)}=\frac{k\times\lambda}{D_{hkl}\times\cos\theta} \quad \text{.....(2.13)}$$

Where

λ the wavelength

2θ is the Bragg angle of reflection

β_L is the integral breadth of the Lorentzian component and β_G is the integral breadth of the Gaussian component [42,43]. From equation (2.7).

2.8 Williamson–Hall Method

The strain induced in powders due to crystal imperfection and distortion was calculated using the formula from equation (2.7), the crystallites size D is less than 1 μ m exhibit profile broadening. The integral breadth in radians is due to the effect of small crystallites is related to D by the equation (2.6) [44]. Strain varies as tanθ, width from crystallite size varies as $\frac{1}{\cos\theta}$, assuming that the particle size and strain contributions to line broadening are separate to each other and both have a Cauchy like profile, the observed line breadth is simply the sum of equations (2.6) and (2.7)[45].

$\beta_{hkl} = \frac{K\lambda}{DCOS\theta} + 4\varepsilon\tan\theta$ ……..……..(2.14)[46].

With C = 4 corresponding to the maximum of strain, multiplying both sides of Eq. (2.14) by cos θ, we obtain [47]. Is regarded as a straight line, y = ax + b. A plot of y = β cosθ against x = sinθ is referred to as the Williamson–hall (W-H) [48]. ε is represented the slope of the straight line while its y intercept is($\frac{K\lambda}{D}$). Equation (2.20) holds true for isotropic line broadening. If both of micro strain profiles and crystallite-size are Gaussian, then the plot is convex downward, having the same terminal slope at a high angle as the Lorentzian case and intercepting the y axis at ($\frac{K\lambda}{D}$), The W-H plot is a very useful diagnostic instrument for learning the kinds of profile broadening and determining approximate values of D and ε [49].

2.9 Alteration Scherrer Method

The equation of the alteration scherrer method is equation (2.6)[50]. And we can determined the width in radian β by separation the above equation, and it is possible to write an equation for the basic Scherrer in this way.

$$\beta = \frac{K\lambda}{D} \cdot \frac{1}{\cos\theta} \quad \text{.....(2.15)}$$

$$\ln\beta = \ln\frac{K\lambda}{D} + \ln\frac{1}{\cos\theta} \quad \text{.....(2.16)}$$

The curve between ln β and the second term of the equation (2.16) must Be obtain the crystallite size and the lattice strain according to the following equation [51,52].

$$e^{\ln\frac{k\lambda}{D}} = e^{intercept} \quad \text{.....(2.17)}$$

2.10 Crystal Structure Parameters

1. Texture Coefficient (TC)

computation of constructing variables to explain the special favored, the texture coefficient $T_c^{(hkl)}$ It is computed using the following formul [53, 54]:

$$T_c^{(hkl)} = [\{(I(hkl)/I_\circ(hkl)\}/\{\frac{1}{Nr}\Sigma I(hkl)/I_\circ(hkl)\}] \times 100\ \% \quad \text{.....(2.18)}$$

Where I(hkl) is the measured relative intensity of a plane hkl, and $I_\circ(hkl)$ the standard intensity of the plane taking from the JCPDS data [55, 56]. Where is the calculated intensity is I, standard intensity is I_o, the number of diffraction peaks Nr and miller indices are hkl.

2. Micro Strains

The micro strains are investigated through the growth of thin films, and will be raised from stretching or compression in the lattice to make a deviation in the a lattice constant so the strain broadening is caused by varying displacements of the atoms with respect to their reference lattice position [57]. This strain can be computation from the formula,

$$< \varepsilon > = \frac{\beta cos\theta}{4} \quad \text{.....(2.19)}$$

Where $\beta$is FWHM (radian), θis Bragg diffraction angle of the XRD peak (degree)[58].

3. Dislocation Density

A dislocation is an flaw in a crystal related in the lattice in one part of the crystal with that in another fraction. Different vacancies and interstitial atoms, dislocations are not equipoise flaw. Thermodynamic thoughts are respect to calculation far their existence in the observed densities. The growth method involving dislocation is a matter of importance [59]. The intrinsic stress and dislocation density are determined by using the X-ray line profile analysis [60,61]. By using equations (2.20) the dislocation density (δ) in the sample has been determined and results from both the formulas are approximately same .

$$\delta = \frac{1}{D^2} \quad \text{.....(2.20)}$$

Where $\delta$is dislocation density, and D is crystallite size (nm). The dislocation density of the sample is inversely proportional to crystallite size[62,63].

4. The Area of the Particle

The stage of the area portray of the nano particles case by the effect of the size and low of this size [64]. And the ship between the area and the size is high the size is low Also the area can be calculate from [65] .

$A = 6*10^3 / D_p \rho$ ……...……..……..……..(2.21)

Where A is the area of the particle and D_P is calculate from manner of method [66] and ρ is take of the MnO (5.39 g.cm) [67].

2.11 New Models

First New Model

Calculation between lattice strain and root- mean strain of Fourier method. From the relation between strain and local root mean- square strain which is,

$< \varepsilon^2 >^{1/2} = (2/\pi)^{1/2} \varepsilon$ ……...……(2.22)

Of calculate the lattice structure for the case of a Gaussian micro strain distribution it is possible to calculate the local root-mean-square strain by using root-mean square strain [68,69].

Second New Model

Through uniform deformation energy density model (UDEDM) can extract energy density of crystal. In equation (2.23) :

$u = \frac{\varepsilon^2}{2} Y_{(hkl)}$ ……..……(2.23)

when the strain energy density u is considered. According to Hooke's law, the constants of proportionality related with the stress and strain relation are no tall autonomous, the energy density u (energy per unit volume) is as a function of strain [44-47].

Third New Model

From uniform stress deformation model (USDM) strain is computed of the Hook's Law preserving line a proportionality between stress and strain by:

$\sigma = Y\,\varepsilon$ ……..……(2.24)

Where σ is the stress and Y is the Young's modulus [47].

Four New Model Of Scherrer Method Modified In Strain

The crystallite size along the (hkl) profile was calculated based on a high resolution x-ray diffraction scan following by the Scherer formula from equation (2.6)[70,71]. In this research, we need to calculate the strain because the first modified Scherrer determined only particle size, therefore we develop this method to obtain the lattices strain by the intercept on the Y- axis. Then the equation of the Scherrer method is developed as the form equation(2.7).

$\ln\beta = \ln 4\varepsilon \frac{sin\theta}{cos\theta}$

$\ln\beta \cos\theta = \ln\varepsilon + \ln 4 \sin\theta$ ……..……...….(2.25)

2.12 Apparent Strain

If the broadening is now due to the sole strain effect, the rapport defined by Stokes and Wilson can be use :

$\varepsilon = \frac{\mu}{4}$ …….. ……..……..…….…….……(2.26)

Where μ is the apparent strain and ε the strain. In almost all cases line broadening occurs due to simultaneously size and lattice distortion effects. One way to separate these two effects has been developed by Williamson and Hall [31] .

Chapter Three
Results and Discussion

3.1 Fourier Analysis Method

The Fourier method was used to analyze x-ray diffraction lines, which is due to MnO nanoparticles figure (2.3) this chart contains five peaks, such as (111), (200) , (220) , (311) and (222) plane respectively for manganese mono oxide (MnO) from Astm card(00-003-1145) with cubic system and face centered cubic lattice. The strong peaks along the plane (200), (111), and (220) designate that the gained product is highly crystalline and has grown in these directions. The figure (3.1) shows the values of h(x) of peak profile (111) which is represents the values of the intensity for each of the twenty steps, ten of which are on the right and the other ten on the left . The beginning and end of the steps were determined by the beginning and end of the x-ray diffraction peak tails.

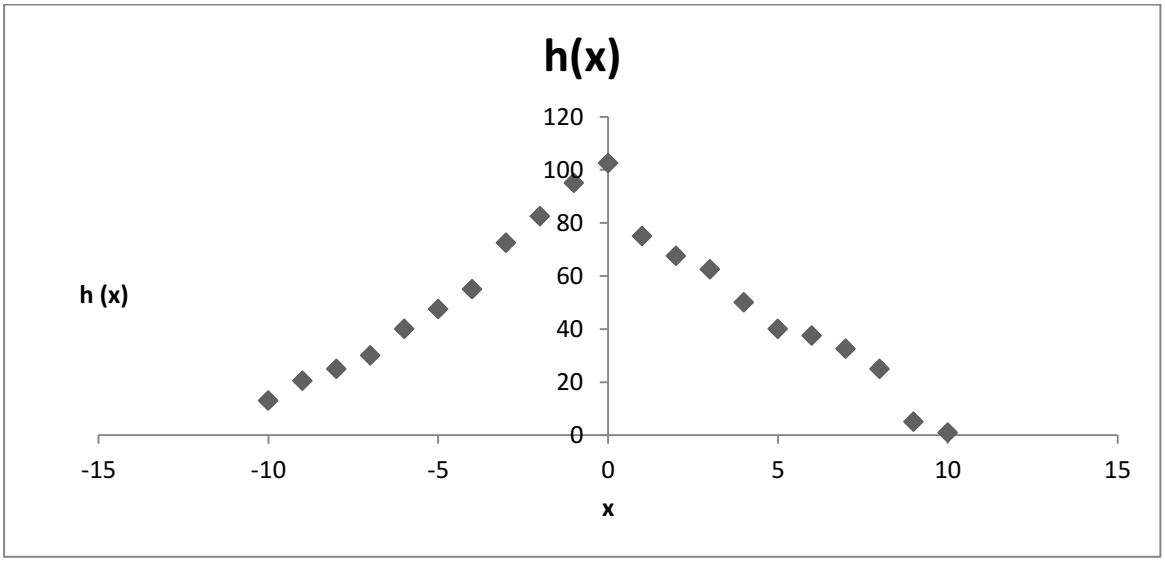

Figure (3.1) : h(x) highs as a function of the distance x of the peak(111)

After h(x) values were collected from right and their values from the left. The average values of Fourier transforms of the true sample Hr (t) were calculated

for different values of variable (t) such as t = 0,1,2,3,4,5,6,7,8,9 and 10 and the result listed in the table (3.1).

Table (3.1) : The values of the integrated intensity profile function for the crystals h(x) for (111) peak and (x) and Fourier transforms of the true sample Hr(t) at all values of Periodic time t from 0 to 10.

at (t=0)

x	h(x)	(2πxt)/60	cos(2πxt)/60	h(x)cos(2πxt)/60	x	h(x)	(2πxt)/60	cos(2πxt)/60	h(x)cos(2πxt)/6	Hr(t)
0	103	0	1	102.5						97.95
1	75	0	1	75	-1	95	0	1	95	
2	68	0	1	67.5	-2	83	0	1	82.5	
3	63	0	1	62.5	-3	73	0	1	72.5	
4	50	0	1	50	-4	55	0	1	55	
5	40	0	1	40	-5	48	0	1	47.5	
6	38	0	1	37.5	-6	40	0	1	40	
7	33	0	1	32.5	-7	30	0	1	30	
8	25	0	1	25	-8	25	0	1	25	
9	5	0	1	5	-9	21	0	1	20.5	
10	1	0	1	1	-10	13	0	1	13	
				498.5					481	

at (t =1)

x	h(x)	(2πxt)/60	cos(2πxt)/60	h(x)cos(2πxt)/60	x	h(x)	(2πxt)/60	cos(2πxt)/60	h(x)cos(2πxt)/6	Hr(t)
0	103	0	1	102.5						88.307
1	75	0.10467	0.9945274	74.58955824	-1	95	-0.1047	0.9945274	94.48010711	
2	68	0.20933	0.9781697	66.02645277	-2	83	-0.2093	0.9781697	80.69899783	
3	63	0.314	0.9511057	59.4441075	-3	73	-0.314	0.9511057	68.9551647	
4	50	0.41867	0.9136318	45.68159046	-4	55	-0.4187	0.9136318	50.2497495	
5	40	0.52333	0.8661581	34.64632378	-5	48	-0.5233	0.8661581	41.14250948	
6	38	0.628	0.8092042	30.34515679	-6	40	-0.628	0.8092042	32.36816724	
7	33	0.73267	0.7433934	24.16028667	-7	30	-0.7327	0.7433934	22.30180308	
8	25	0.83733	0.6694462	16.73615413	-8	25	-0.8373	0.6694462	16.73615413	
9	5	0.942	0.5881717	2.940858652	-9	21	-0.942	0.5881717	12.05752047	
10	1	1.04667	0.5004597	0.500459689	-10	13	-1.0467	0.5004597	6.505975957	
				457.5709487					425.4961495	

at (t=2)

x	h(x)	(2πxt)/60	cos(2πxt)/60	h(x)cos(2πxt)/60	x	h(x)	(2πxt)/60	cos(2πxt)/60	h(x)cos(2πxt)/6	Hr(t)
0	103	0	1	102.5						63.971
1	75	0.20933	0.9781697	73.3627253	-1	95	-0.2093	0.9781697	92.92611871	
2	68	0.41867	0.9136318	61.67014712	-2	83	-0.4187	0.9136318	75.37462425	
3	63	0.628	0.8092042	50.57526131	-3	73	-0.628	0.8092042	58.66730312	
4	50	0.83733	0.6694462	33.47230826	-4	55	-0.8373	0.6694462	36.81953909	
5	40	1.04667	0.5004597	20.01838756	-5	48	-1.0467	0.5004597	23.77183523	
6	38	1.256	0.3096228	11.61085549	-6	40	-1.256	0.3096228	12.38491252	
7	33	1.46533	0.1052676	3.421197037	-7	30	-1.4653	0.1052676	3.158028034	
8	25	1.67467	-0.1036837	-2.59209159	-8	25	-1.6747	-0.103684	-2.59209159	
9	5	1.884	-0.308108	-1.540540156	-9	21	-1.884	-0.308108	-6.316214641	
10	1	2.09333	-0.4990802	-0.499080199	-10	13	-2.0933	-0.49908	-6.488042592	
				351.9991701					287.7060121	

at (t=3)

x	h(x)	(2πxt)/60	cos(2πxt)/60	h(x)cos(2πxt)/60	x	h(x)	(2πxt)/60	cos(2πxt)/60	h(x)cos(2πxt)/6	Hr(t)
0	103	0	1	102.5						35.834
1	75	0.314	0.9511057	71.332929	-1	95	-0.314	0.9511057	90.35504339	
2	68	0.628	0.8092042	54.62128222	-2	83	-0.628	0.8092042	66.75934493	
3	63	0.942	0.5881717	36.76073315	-3	73	-0.942	0.5881717	42.64245045	
4	50	1.256	0.3096228	15.48114065	-4	55	-1.256	0.3096228	17.02925472	
5	40	1.57	0.0007963	0.031853068	-5	48	-1.57	0.0007963	0.037825519	
6	38	1.884	-0.308108	-11.55405117	-6	40	-1.884	-0.308108	-12.32432125	
7	33	2.198	-0.5868829	-19.07369583	-7	30	-2.198	-0.586883	-17.60648846	
8	25	2.512	-0.8082674	-20.20668568	-8	25	-2.512	-0.808267	-20.20668568	
9	5	2.826	-0.9506126	-4.753062991	-9	21	-2.826	-0.950613	-19.48755826	
10	1	3.14	-0.9999987	-0.999998732	-10	13	-3.14	-0.999999	-12.99998351	
				224.1404437					134.1988818	

at (t=4)

x	h(x)	(2πxt)/60	cos(2πxt)/60	h(x)cos(2πxt)/60	x	h(x)	(2πxt)/60	cos(2πxt)/60	h(x)cos(2πxt)/6	Hr(t)
0	103	0	1	102.5						14.511
1	75	0.41867	0.9136318	68.52238568	-1	95	-0.4187	0.9136318	86.79502187	
2	68	0.83733	0.6694462	45.18761616	-2	83	-0.8373	0.6694462	55.22930864	
3	63	1.256	0.3096228	19.35142582	-3	73	-1.256	0.3096228	22.44765395	
4	50	1.67467	-0.1036837	-5.18418318	-4	55	-1.6747	-0.103684	-5.702601498	
5	40	2.09333	-0.4990802	-19.96320797	-5	48	-2.0933	-0.49908	-23.70630947	
6	38	2.512	-0.8082674	-30.31002852	-6	40	-2.512	-0.808267	-32.33069709	
7	33	2.93067	-0.9778375	-31.77971759	-7	30	-2.9307	-0.977837	-29.33512393	
8	25	3.34933	-0.9784994	-24.4624849	-8	25	-3.3493	-0.978499	-24.4624849	
9	5	3.768	-0.8101389	-4.050694411	-9	21	-3.768	-0.810139	-16.60784708	
10	1	4.18667	-0.5018379	-0.501837909	-10	13	-4.1867	-0.501838	-6.52389282	
				119.3092732					25.80302766	

at(t=5)

x	h(x)	(2πxt)/60	cos(2πxt)/60	h(x)cos(2πxt)/60	x	h(x)	(2πxt)/60	cos(2πxt)/60	h(x)cos(2πxt)/6	Hr(t)
0	103	0	1	102.5						4.6931
1	75	0.52333	0.8661581	64.96185708	-1	95	-0.5233	0.8661581	82.28501897	
2	68	1.04667	0.5004597	33.78102901	-2	83	-1.0467	0.5004597	41.28792434	
3	63	1.57	0.0007963	0.049770419	-3	73	-1.57	0.0007963	0.057733687	
4	50	2.09333	-0.4990802	-24.95400997	-4	55	-2.0933	-0.49908	-27.44941096	
5	40	2.61667	-0.865361	-34.61444142	-5	48	-2.6167	-0.865361	-41.10464919	
6	38	3.14	-0.9999987	-37.49995244	-6	40	-3.14	-0.999999	-39.99994927	
7	33	3.66333	-0.866953	-28.17597108	-7	30	-3.6633	-0.866953	-26.00858869	
8	25	4.18667	-0.5018379	-12.54594773	-8	25	-4.1867	-0.501838	-12.54594773	
9	5	4.71	-0.002389	-0.011944891	-9	21	-4.71	-0.002389	-0.048974051	
10	1	5.23333	0.4976994	0.497699444	-10	13	-5.2333	0.4976994	6.470092769	
				63.98808842					-17.05675012	

at (t=6)

x	h(x)	(2πxt)/60	cos(2πxt)/60	h(x)cos(2πxt)/60	x	h(x)	(2πxt)/60	cos(2πxt)/60	h(x)cos(2πxt)/6	Hr(t)
0	103	0	1	102.5						4.023
1	75	0.628	0.8092042	60.69031357	-1	95	-0.628	0.8092042	76.87439719	
2	68	1.256	0.3096228	20.89953988	-2	83	-1.256	0.3096228	25.54388208	
3	63	1.884	-0.308108	-19.25675195	-3	73	-1.884	-0.308108	-22.33783227	
4	50	2.512	-0.8082674	-40.41337136	-4	55	-2.512	-0.808267	-44.4547085	
5	40	3.14	-0.9999987	-39.99994927	-5	48	-3.14	-0.999999	-47.49993976	
6	38	3.768	-0.8101389	-30.38020808	-6	40	-3.768	-0.810139	-32.40555528	
7	33	4.396	-0.3111368	-10.11194631	-7	30	-4.396	-0.311137	-9.334104284	
8	25	5.024	0.3065925	7.664811699	-8	25	-5.024	0.3065925	7.664811699	
9	5	5.652	0.8073286	4.036643117	-9	21	-5.652	0.8073286	16.55023678	
10	1	6.28	0.9999949	0.999994927	-10	13	-6.28	0.9999949	12.99993405	
				56.62907622					-16.39887829	

at (t=7)

x	h(x)	(2πxt)/60	cos(2πxt)/60	h(x)cos(2πxt)/60	x	h(x)	(2πxt)/60	cos(2πxt)/60	h(x)cos(2πxt)/6	Hr(t)
0	103	0	1	102.5						6.5006
1	75	0.73267	0.7433934	55.75450769	-1	95	-0.7327	0.7433934	70.62237641	
2	68	1.46533	0.1052676	7.105563076	-2	83	-1.4653	0.1052676	8.684577093	
3	63	2.198	-0.5868829	-36.68018428	-3	73	-2.198	-0.586883	-42.54901377	
4	50	2.93067	-0.9778375	-48.89187322	-4	55	-2.9307	-0.977837	-53.78106054	
5	40	3.66333	-0.866953	-34.67811825	-5	48	-3.6633	-0.866953	-41.18026542	
6	38	4.396	-0.3111368	-11.66763035	-6	40	-4.396	-0.311137	-12.44547238	
7	33	5.12867	0.4043588	13.14166206	-7	30	-5.1287	0.4043588	12.13076498	
8	25	5.86133	0.9123322	22.80830533	-8	25	-5.8613	0.9123322	22.80830533	
9	5	6.594	0.9520847	4.760423624	-9	21	-6.594	0.9520847	19.51773686	
10	1	7.32667	0.5032149	0.503214857	-10	13	-7.3267	0.5032149	6.541793135	
				74.65587054					-9.650258298	

at (t=8)

x	h(x)	(2πxt)/60	cos(2πxt)/60	h(x)cos(2πxt)/60	x	h(x)	(2πxt)/60	cos(2πxt)/60	h(x)cos(2πxt)/6	Hr(t)
0	103	0	1	102.5						7.2536
1	75	0.83733	0.6694462	50.2084624	-1	95	-0.8373	0.6694462	63.5973857	
2	68	1.67467	-0.1036837	-6.998647293	-2	83	-1.6747	-0.103684	-8.553902247	
3	63	2.512	-0.8082674	-50.5167142	-3	73	-2.512	-0.808267	-58.59938848	
4	50	3.34933	-0.9784994	-48.92496979	-4	55	-3.3493	-0.978499	-53.81746677	
5	40	4.18667	-0.5018379	-20.07351637	-5	48	-4.1867	-0.501838	-23.83730069	
6	38	5.024	0.3065925	11.49721755	-6	40	-5.024	0.3065925	12.26369872	
7	33	5.86133	0.9123322	29.65079693	-7	30	-5.8613	0.9123322	27.3699664	
8	25	6.69867	0.9149221	22.87305338	-8	25	-6.6987	0.9149221	22.87305338	
9	5	7.536	0.31265	1.563250083	-9	21	-7.536	0.31265	6.409325341	
10	1	8.37333	-0.4963174	-0.496317426	-10	13	-8.3733	-0.496317	-6.452126535	
				91.28261525					-18.74675518	

at(t=9)

x	h(x)	(2πxt)/60	cos(2πxt)/60	h(x)cos(2πxt)/60	x	h(x)	(2πxt)/60	cos(2πxt)/60	h(x)cos(2πxt)/6	Hr(t)
0	103	0	1	102.5						5.1473
1	75	0.942	0.5881717	44.11287977	-1	95	-0.942	0.5881717	55.87631438	
2	68	1.884	-0.308108	-20.79729211	-2	83	-1.884	-0.308108	-25.41891258	
3	63	2.826	-0.9506126	-59.41328738	-3	73	-2.826	-0.950613	-68.91941336	
4	50	3.768	-0.8101389	-40.50694411	-4	55	-3.768	-0.810139	-44.55763852	
5	40	4.71	-0.002389	-0.095559124	-5	48	-4.71	-0.002389	-0.11347646	
6	38	5.652	0.8073286	30.27482338	-6	40	-5.652	0.8073286	32.29314493	
7	33	6.594	0.9520847	30.94275356	-7	30	-6.594	0.9520847	28.56254174	
8	25	7.536	0.31265	7.816250416	-8	25	-7.536	0.31265	7.816250416	
9	5	8.478	-0.5843009	-2.921504611	-9	21	-8.478	-0.584301	-11.97816891	
10	1	9.42	-0.9999886	-0.999988586	-10	13	-9.42	-0.999989	-12.99985161	
				90.9121312					-39.43920996	

at(t=10)

x	h(x)	(2πxt)/60	cos(2πxt)/60	h(x)cos(2πxt)/60	x	h(x)	(2πxt)/60	cos(2πxt)/60	h(x)cos(2πxt)/60	Hr(t)
0	102.5	0	1	102.5						2.01
1	75	1.046666667	0.500459689	37.53447668	-1	95	-1.0466667	0.500459689	47.54367046	
2	67.5	2.093333333	-0.499080199	-33.68791346	-2	82.5	-2.0933333	-0.499080199	-41.17411645	
3	62.5	3.14	-0.999998732	-62.49992073	-3	72.5	-3.14	-0.999998732	-72.49990805	
4	50	4.186666667	-0.501837909	-25.09189546	-4	55	-4.1866667	-0.501837909	-27.60108501	
5	40	5.233333333	0.497699444	19.90797775	-5	47.5	-5.2333333	0.497699444	23.64072358	
6	37.5	6.28	0.999994927	37.49980976	-6	40	-6.28	0.999994927	39.99979708	
7	32.5	7.326666667	0.503214857	16.35448284	-7	30	-7.3266667	0.503214857	15.0964457	
8	25	8.373333333	-0.496317426	-12.40793564	-8	25	-8.3733333	-0.496317426	-12.40793564	
9	5	9.42	-0.999988586	-4.999942928	-9	20.5	-9.42	-0.999988586	-20.499766	
10	1	10.46666667	-0.504590527	-0.504590527	-10	13	-10.466667	-0.504590527	-6.559676856	
				74.60454827					-54.4618512	

Find a value (Hr) by applying the equation below to the tables.

$Hr = 0.1\sum h(x)\cos(2\pi xt)/60.$

The values of standard sample g(x) of peak profile which is represent the values of the intensity for each of the twenty steps, ten of which are on the right and the other ten on the left for the line of diffraction that returns to the standard model and usually uses quartz as a single crystal. The ten values of g(x). Each value was obtained for one value of (t) and g(x) values were obtained for Fourier transforms of the standard Gr(t) and the results are listed in Table (3.2).

Table (3.2) : The values of standard sample g(x) for standard peak and (x) and Fourier transforms of the standard Gr(t) at all values of periodic time t from 0 to 10.

at(t=0)

x	g(x)	(2πxt)/60	cos(2πxt)/60	g(x)cos(2πxt)/60	x	g(x)	(2πxt)/60	cos(2πxt)/60	g(x)cos(2πxt)/60	Gr(t)
0	350	0	1	350						310
1	330	0	1	330	-1	320	0	1	320	
2	300	0	1	300	-2	290	0	1	290	
3	200	0	1	200	-3	225	0	1	225	
4	160	0	1	160	-4	150	0	1	150	
5	125	0	1	125	-5	130	0	1	130	
6	105	0	1	105	-6	75	0	1	75	
7	85	0	1	85	-7	45	0	1	45	
8	70	0	1	70	-8	25	0	1	25	
9	50	0	1	50	-9	20	0	1	20	
10	35	0	1	35	-10	10	0	1	10	
				1810					1290	

at (t=1)

x	g(x)	(2πxt)/60	cos(2πxt)/60	g(x)cos(2πxt)/60	x	g(x)	(2πxt)/60	cos(2πxt)/60	g(x)cos(2πxt)/60	Gr(t)
0	350	0	1	350						285.1
1	330	0.1046667	0.994527443	328.1940563	-1	320	-0.1046667	0.994527443	318.2487818	
2	300	0.2093333	0.978169671	293.4509012	-2	290	-0.2093333	0.978169671	283.6692045	
3	200	0.314	0.95110572	190.221144	-3	225	-0.314	0.95110572	213.998787	
4	160	0.4186667	0.913631809	146.1810895	-4	150	-0.4186667	0.913631809	137.0447714	
5	125	0.5233333	0.866158094	108.2697618	-5	130	-0.5233333	0.866158094	112.6005523	
6	105	0.628	0.809204181	84.966439	-6	75	-0.628	0.809204181	60.69031357	
7	85	0.7326667	0.743393436	63.18844205	-7	45	-0.7326667	0.743393436	33.45270462	
8	70	0.8373333	0.669446165	46.86123157	-8	25	-0.8373333	0.669446165	16.73615413	
9	50	0.942	0.58817173	29.40858652	-9	20	-0.942	0.58817173	11.76343461	
10	35	1.0466667	0.500459689	17.51608912	-10	10	-1.0466667	0.500459689	5.00459689	
				1658.257741					1193.209301	

at (t=2)

x	g(x)	(2πxt)/60	cos(2πxt)/60	g(x)cos(2πxt)/60	x	g(x)	(2πxt)/60	cos(2πxt)/60	g(x)cos(2πxt)/60	Gr(t)
0	350	0	1	350						221.9
1	330	0.20933333	0.978169671	322.7959913	-1	320	-0.2093333	0.978169671	313.0142946	
2	300	0.41866667	0.913631809	274.0895427	-2	290	-0.4186667	0.913631809	264.9532246	
3	200	0.628	0.809204181	161.8408362	-3	225	-0.628	0.809204181	182.0709407	
4	160	0.83733333	0.669446165	107.1113864	-4	150	-0.8373333	0.669446165	100.4169248	
5	125	1.04666667	0.500459689	62.55746113	-5	130	-1.0466667	0.500459689	65.05975957	
6	105	1.256	0.309622813	32.51039537	-6	75	-1.256	0.309622813	23.22171098	
7	85	1.46533333	0.105267601	8.947746096	-7	45	-1.4653333	0.105267601	4.737042051	
8	70	1.67466667	-0.10368366	-7.257856452	-8	25	-1.6746667	-0.103683664	-2.59209159	
9	50	1.884	-0.30810803	-15.40540156	-9	20	-1.884	-0.308108031	-6.162160626	
10	35	2.09333333	-0.4990802	-17.46780698	-10	10	-2.0933333	-0.499080199	-4.990801994	
				1279.722294					939.7288432	

at(t=3)

x	g(x)	(2πxt)/60	cos(2πxt)/60	g(x)cos(2πxt)/60	x	g(x)	(2πxt)/60	cos(2πxt)/60	g(x)cos(2πxt)/60	Gr(t)
0	350	0	1	350						147.17
1	330	0.314	0.9511057	313.8648876	-1	320	-0.314	0.95110572	304.3538304	
2	300	0.628	0.8092042	242.7612543	-2	290	-0.628	0.80920418	234.6692125	
3	200	0.942	0.5881717	117.6343461	-3	225	-0.942	0.58817173	132.3386393	
4	160	1.256	0.3096228	49.53965009	-4	150	-1.256	0.30962281	46.44342196	
5	125	1.57	0.0007963	0.099540839	-5	130	-1.57	0.00079633	0.103522472	
6	105	1.884	-0.308108	-32.35134328	-6	75	-1.884	-0.308108	-23.10810235	
7	85	2.198	-0.586883	-49.88505062	-7	45	-2.198	-0.5868829	-26.40973268	
8	70	2.512	-0.808267	-56.57871991	-8	25	-2.512	-0.8082674	-20.20668568	
9	50	2.826	-0.950613	-47.53062991	-9	20	-2.826	-0.9506126	-19.01225196	
10	35	3.14	-0.999999	-34.99995561	-10	10	-3.14	-0.9999987	-9.999987317	
				852.5539795					619.1718666	

at(t=4)

x	g(x)	(2πxt)/60	cos(2πxt)/60	g(x)cos(2πxt)/60	x	g(x)	(2πxt)/60	cos(2πxt)/60	g(x)cos(2πxt)/60	Gr(t)
0	350	0	1	350						86.6
1	330	0.4187	0.913632	301.498497	-1	320	-0.419	0.91363181	292.3621789	
2	300	0.8373	0.669446	200.8338496	-2	290	-0.837	0.66944617	194.1393879	
3	200	1.256	0.309623	61.92456261	-3	225	-1.256	0.30962281	69.66513294	
4	160	1.6747	-0.103684	-16.58938618	-4	150	-1.675	-0.1036837	-15.55254954	
5	125	2.0933	-0.49908	-62.38502492	-5	130	-2.093	-0.4990802	-64.88042592	
6	105	2.512	-0.808267	-84.86807986	-6	75	-2.512	-0.8082674	-60.62005705	
7	85	2.9307	-0.977837	-83.11618447	-7	45	-2.931	-0.9778375	-44.00268589	
8	70	3.3493	-0.978499	-68.49495771	-8	25	-3.349	-0.9784994	-24.4624849	
9	50	3.768	-0.810139	-40.50694411	-9	20	-3.768	-0.8101389	-16.20277764	
10	35	4.1867	-0.501838	-17.56432682	-10	10	-4.187	-0.5018379	-5.018379092	
				540.7320051					325.4273398	

at (t=5)

x	g(x)	(2πxt)/60	cos(2πxt)/60	g(x)cos(2πxt)/60	x	g(x)	(2πxt)/60	cos(2πxt)/60	g(x)cos(2πxt)/60	Gr(t)
0	350	0	1	350						51.51
1	330	0.5233	0.8661581	285.8321712	-1	320	-0.523	0.86615809	277.1705902	
2	300	1.0467	0.5004597	150.1379067	-2	290	-1.047	0.50045969	145.1333098	
3	200	1.57	0.0007963	0.159265342	-3	225	-1.57	0.00079633	0.17917351	
4	160	2.0933	-0.49908	-79.8528319	-4	150	-2.093	-0.4990802	-74.8620299	
5	125	2.6167	-0.865361	-108.1701294	-5	130	-2.617	-0.865361	-112.4969346	
6	105	3.14	-0.999999	-104.9998668	-6	75	-3.14	-0.9999987	-74.99990488	
7	85	3.6633	-0.866953	-73.69100128	-7	45	-3.663	-0.866953	-39.01288303	
8	70	4.1867	-0.501838	-35.12865365	-8	25	-4.187	-0.5018379	-12.54594773	
9	50	4.71	-0.002389	-0.119448906	-9	20	-4.71	-0.002389	-0.047779562	
10	35	5.2333	0.4976994	17.41948053	-10	10	-5.233	0.49769944	4.976994438	
				401.5868917					113.4945882	

at(t=6)

x	g(x)	(2πxt)/60	cos(2πxt)/60	g(x)cos(2πxt)/60	x	g(x)	(2πxt)/60	cos(2πxt)/60	g(x)cos(2πxt)/60	Gr(t)
0	350	0	1	350						36.652
1	330	0.628	0.8092042	267.0373797	-1	320	-0.628	0.80920418	258.9453379	
2	300	1.256	0.3096228	92.88684392	-2	290	-1.256	0.30962281	89.79061579	
3	200	1.884	-0.308108	-61.62160626	-3	225	-1.884	-0.308108	-69.32430704	
4	160	2.512	-0.808267	-129.3227884	-4	150	-2.512	-0.8082674	-121.2401141	
5	125	3.14	-0.999999	-124.9998415	-5	130	-3.14	-0.9999987	-129.9998351	
6	105	3.768	-0.810139	-85.06458262	-6	75	-3.768	-0.8101389	-60.76041616	
7	85	4.396	-0.311137	-26.4466288	-7	45	-4.396	-0.3111368	-14.00115643	
8	70	5.024	0.3065925	21.46147276	-8	25	-5.024	0.30659247	7.664811699	
9	50	5.652	0.8073286	40.36643117	-9	20	-5.652	0.80732862	16.14657247	
10	35	6.28	0.9999949	34.99982244	-10	10	-6.28	0.99999493	9.999949269	
				379.2965025					-12.7785417	

at (t=7)

x	g(x)	(2πxt)/60	cos(2πxt)/60	g(x)cos(2πxt)/60	x	g(x)	(2πxt)/60	cos(2πxt)/60	g(x)cos(2πxt)/60	Gr(t)
0	350	0	1	350						29.42
1	330	0.73267	0.7433934	245.3198339	-1	320	-0.7327	0.7433934	237.8858995	
2	300	1.46533	0.1052676	31.58028034	-2	290	-1.4653	0.1052676	30.52760433	
3	200	2.198	-0.586883	-117.3765897	-3	225	-2.198	-0.586883	-132.0486634	
4	160	2.93067	-0.977837	-156.4539943	-4	150	-2.9307	-0.977837	-146.6756196	
5	125	3.66333	-0.866953	-108.3691195	-5	130	-3.6633	-0.866953	-112.7038843	
6	105	4.396	-0.311137	-32.66936499	-6	75	-4.396	-0.311137	-23.33526071	
7	85	5.12867	0.4043588	34.37050077	-7	45	-5.1287	0.4043588	18.19614746	
8	70	5.86133	0.9123322	63.86325492	-8	25	-5.8613	0.9123322	22.80830533	
9	50	6.594	0.9520847	47.60423624	-9	20	-6.594	0.9520847	19.0416945	
10	35	7.32667	0.5032149	17.61251998	-10	10	-7.3267	0.5032149	5.032148565	
				375.4815576					-81.2716284	

at (t=8)

x	g(x)	(2πxt)/60	cos(2πxt)/60	(x)cos(2πxt)/60	x	g(x)	(2πxt)/60	cos(2πxt)/60	(x)cos(2πxt)/6	Gr(t)
0	350	0	1	350						20.94
1	330	0.8373	0.6694462	220.9172345	-1	320	-0.8373	0.66944617	214.2227729	
2	300	1.6747	-0.1036837	-31.10509908	-2	290	-1.6747	-0.10368366	-30.0682624	
3	200	2.512	-0.8082674	-161.6534855	-3	225	-2.512	-0.80826743	-181.860171	
4	160	3.3493	-0.9784994	-156.5599033	-4	150	-3.3493	-0.9784994	-146.774909	
5	125	4.1867	-0.5018379	-62.72973865	-5	130	-4.1867	-0.50183791	-65.2389282	
6	105	5.024	0.3065925	32.19220914	-6	75	-5.024	0.30659247	22.9944351	
7	85	5.8613	0.9123322	77.54823812	-7	45	-5.8613	0.91233221	41.05494959	
8	70	6.6987	0.9149221	64.04454946	-8	25	-6.6987	0.91492214	22.87305338	
9	50	7.536	0.31265	15.63250083	-9	20	-7.536	0.31265002	6.253000333	
10	35	8.3733	-0.4963174	-17.3711099	-10	10	-8.3733	-0.49631743	-4.96317426	
				330.9153957					-121.507234	

at (t=9)

x	g(x)	(2πxt)/60	cos(2πxt)/60	g(x)cos(2πxt)/60	x	g(x)	(2πxt)/60	cos(2πxt)/60	g(x)cos(2πxt)/60	Gr(t)
0	350	0	1	350						10.77
1	330	0.942	0.5881717	194.096671	-1	320	-0.942	0.58817173	188.2149537	
2	300	1.884	-0.308108	-92.43240938	-2	290	-1.884	-0.308108	-89.35132907	
3	200	2.826	-0.950613	-190.1225196	-3	225	-2.826	-0.9506126	-213.8878346	
4	160	3.768	-0.810139	-129.6222211	-4	150	-3.768	-0.8101389	-121.5208323	
5	125	4.71	-0.002389	-0.298622264	-5	130	-4.71	-0.002389	-0.310567155	
6	105	5.652	0.8073286	84.76950545	-6	75	-5.652	0.80732862	60.54964675	
7	85	6.594	0.9520847	80.92720161	-7	45	-6.594	0.95208472	42.84381262	
8	70	7.536	0.31265	21.88550117	-8	25	-7.536	0.31265002	7.816250416	
9	50	8.478	-0.584301	-29.21504611	-9	20	-8.478	-0.5843009	-11.68601844	
10	35	9.42	-0.999989	-34.99960049	-10	10	-9.42	-0.9999886	-9.999885856	
				254.9884602					-147.3318039	

at (t=10)

x	g(x)	(2πxt)/60	cos(2πxt)/60	g(x)cos(2πxt)/60	x	g(x)	(2πxt)/60	cos(2πxt)/60	g(x)cos(2πxt)/60	Gr(t)
0	350	0	1	350						3.2747
1	330	1.0467	0.5004597	165.1516974	-1	320	-1.047	0.50045969	160.1471005	
2	300	2.0933	-0.49908	-149.7240598	-2	290	-2.093	-0.4990802	-144.7332578	
3	200	3.14	-0.999999	-199.9997463	-3	225	-3.14	-0.9999987	-224.9997146	
4	160	4.1867	-0.501838	-80.29406548	-4	150	-4.187	-0.5018379	-75.27568638	
5	125	5.2333	0.4976994	62.21243047	-5	130	-5.233	0.49769944	64.70092769	
6	105	6.28	0.9999949	104.9994673	-6	75	-6.28	0.99999493	74.99961952	
7	85	7.3267	0.5032149	42.7732628	-7	45	-7.327	0.50321486	22.64466854	
8	70	8.3733	-0.496317	-34.7422198	-8	25	-8.373	-0.4963174	-12.40793564	
9	50	9.42	-0.999989	-49.99942928	-9	20	-9.42	-0.9999886	-19.99977171	
10	35	10.467	-0.504591	-17.66066846	-10	10	-10.47	-0.5045905	-5.045905274	
				192.7166688					-159.9699552	

Find a value Fourier transforms of the standard sample (Gr) by applying the equation below to the tables.

$$Gr = 0.1\sum g(x)\cos(2\pi xt)/60.$$

Table (3.3) : The values of Fourier transforms F(L), H(L) and G(L) values of (t) of the peak (111) .

t	Hr(t)	Gr(t)	Fr(t)
0	97.95	310	0.315967742
1	88.30670982	285	0.309848105
2	63.97051823	221.9451137	0.288226747
3	35.83393255	147.1725846	0.243482389
4	14.51123008	86.61593449	0.167535341
5	4.69313383	51.508148	0.091114397
6	4.023019793	36.65179608	0.109763237
7	6.500561224	29.42099292	0.220949757
8	7.253586007	20.94081616	0.346385067
9	5.147292124	10.76566563	0.478121121
10	2.014269707	3.274671358	0.61510591
			0.318649981

Equation (2.9) was used to calculate the value Fourier transforms Fr (t) for each value of Fourier transforms of the true sample Hr(t) and Fourier transforms of the standard sample Gr(t) , and the results were included in the Table (3.3).

The figure (3.2) shows the values of the intensity is represented by the integrated intensity profile function for the crystals h(x) of line profile(200) for the steps, at the values of (t).

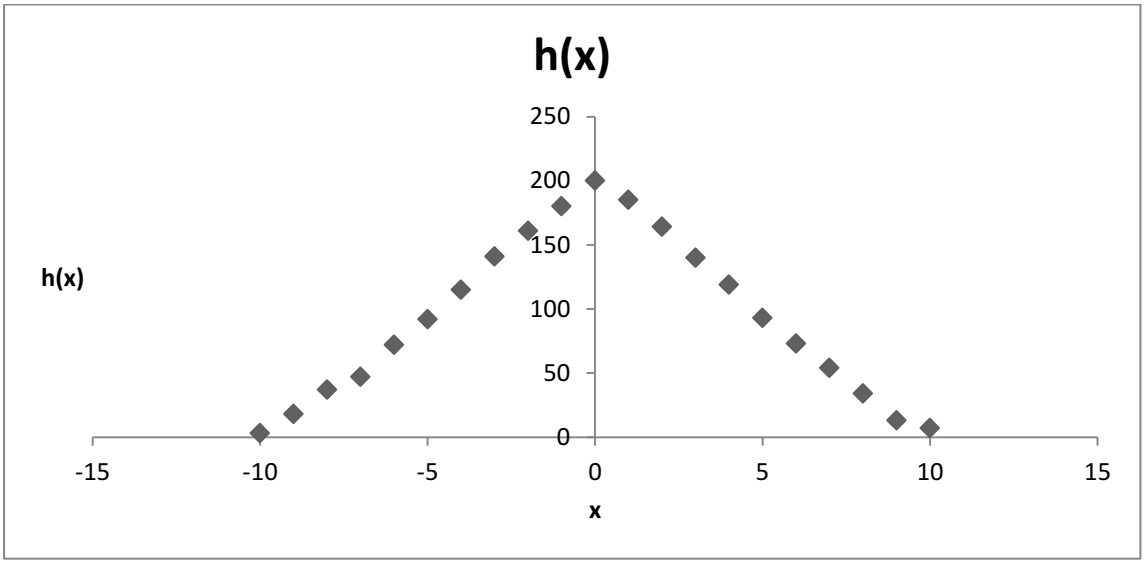

Figure (3.2) : h(x) highs as a function of the distance x of the peak(200).

All of The values of the integrated intensity profile function for the crystals h(x) and x are set in table (3.4) to calculate one value of Fourier transforms of the true sample Hr(t) for any value of (t).

Table (3.4) : The values of the integrated intensity profile function for the crystals h(x) for (200) peak and (x) and Fourier transforms of the true sample Hr(t) at all values of periodic time t from 0 to 10.

a(t=0)

x	h(x)	(2πxt)/60	cos(2πxt)/60	h(x)cos(2πxt)/60	x	h(x)	(2πxt)/60	cos(2πxt)/60	h(x)cos(2πxt)/60	Hr(t)
0	200	0	1	200						194.8
1	185	0	1	185	-1	180	0	1	180	
2	164	0	1	164	-2	161	0	1	161	
3	140	0	1	140	-3	141	0	1	141	
4	119	0	1	119	-4	115	0	1	115	
5	93	0	1	93	-5	92	0	1	92	
6	73	0	1	73	-6	72	0	1	72	
7	54	0	1	54	-7	47	0	1	47	
8	34	0	1	34	-8	37	0	1	37	
9	13	0	1	13	-9	18	0	1	18	
10	7	0	1	7	-10	3	0	1	3	
				1082					866	

at (t=1)

x	h(x)	(2πxt)/60	cos(2πxt)/60	h(x)cos(2πxt)/60	x	h(x)	(2πxt)/60	cos(2πxt)/60	h(x)cos(2πxt)/60	Hr(t)
0	200	0	1	200						178.538
1	185	0.1047	0.9945274	183.987577	-1	180	-0.1047	0.9945274	179.0149398	
2	164	0.2093	0.9781697	160.419826	-2	161	-0.2093	0.9781697	157.485317	
3	140	0.314	0.9511057	133.1548008	-3	141	-0.314	0.9511057	134.1059065	
4	119	0.4187	0.9136318	108.7221853	-4	115	-0.4187	0.9136318	105.067658	
5	93	0.5233	0.8661581	80.55270278	-5	92	-0.5233	0.8661581	79.68654469	
6	73	0.628	0.8092042	59.07190521	-6	72	-0.628	0.8092042	58.26270103	
7	54	0.7327	0.7433934	40.14324554	-7	47	-0.7327	0.7433934	34.93949149	
8	34	0.8373	0.6694462	22.76116962	-8	37	-0.8373	0.6694462	24.76950812	
9	13	0.942	0.5881717	7.646232494	-9	18	-0.942	0.5881717	10.58709115	
10	7	1.0467	0.5004597	3.503217823	-10	3	-1.0467	0.5004597	1.501379067	
				999.9628625					785.4205368	

at (t=2)

x	h(x)	(2πxt)/60	cos(2πxt)/60	h(x)cos(2πxt)/60	x	h(x)	(2πxt)/60	cos(2πxt)/60	h(x)cos(2πxt)/60	Hr(t)
0	200	0	1	200						136.421
1	185	0.2093	0.9781697	180.9613891	-1	180	-0.2093	0.9781697	176.0705407	
2	164	0.4187	0.9136318	149.8356167	-2	161	-0.4187	0.9136318	147.0947213	
3	140	0.628	0.8092042	113.2885853	-3	141	-0.628	0.8092042	114.0977895	
4	119	0.8373	0.6694462	79.66409367	-4	115	-0.8373	0.6694462	76.98630901	
5	93	1.0467	0.5004597	46.54275108	-5	92	-1.0467	0.5004597	46.04229139	
6	73	1.256	0.3096228	22.60246535	-6	72	-1.256	0.3096228	22.29284254	
7	54	1.4653	0.1052676	5.684450461	-7	47	-1.4653	0.1052676	4.947577253	
8	34	1.6747	-0.1036837	-3.525244562	-8	37	-1.6747	-0.1036837	-3.836295553	
9	13	1.884	-0.308108	-4.005404407	-9	18	-1.884	-0.308108	-5.545944563	
10	7	2.0933	-0.4990802	-3.493561395	-10	3	-2.0933	-0.4990802	-1.497240598	
				787.5551413					576.652591	

at (t=3)

x	h(x)	(2πxt)/60	cos(2πxt)/60	h(x)cos(2πxt)/60	x	h(x)	(2πxt)/60	cos(2πxt)/60	h(x)cos(2πxt)/60	Hr(t)
0	200	0	1	200						84.7213
1	185	0.314	0.9511057	175.9545582	-1	180	-0.314	0.9511057	171.1990296	
2	164	0.628	0.8092042	132.7094857	-2	161	-0.628	0.8092042	130.2818731	
3	140	0.942	0.5881717	82.34404225	-3	141	-0.942	0.5881717	82.93221398	
4	119	1.256	0.3096228	36.84511475	-4	115	-1.256	0.3096228	35.6066235	
5	93	1.57	0.0007963	0.074058384	-5	92	-1.57	0.0007963	0.073262057	
6	73	1.884	-0.308108	-22.49188628	-6	72	-1.884	-0.308108	-22.18377825	
7	54	2.198	-0.5868829	-31.69167922	-7	47	-2.198	-0.5868829	-27.58349858	
8	34	2.512	-0.8082674	-27.48109253	-8	37	-2.512	-0.8082674	-29.90589481	
9	13	2.826	-0.9506126	-12.35796378	-9	18	-2.826	-0.9506126	-17.11102677	
10	7	3.14	-0.9999987	-6.999991122	-10	3	-3.14	-0.9999987	-2.999996195	
				526.9046463					320.3088077	

at (t=4)

x	h(x)	(2πxt)/60	cos(2πxt)/60	h(x)cos(2πxt)/60	x	h(x)	(2πxt)/60	cos(2πxt)/60	h(x)cos(2πxt)/60	Hr(t)
0	200	0	1	200						40.5891
1	185	0.4187	0.9136318	169.0218847	-1	180	-0.4187	0.9136318	164.4537256	
2	164	0.8373	0.6694462	109.7891711	-2	161	-0.8373	0.6694462	107.7808326	
3	140	1.256	0.3096228	43.34719383	-3	141	-1.256	0.3096228	43.65681664	
4	119	1.6747	-0.1036837	-12.33835597	-4	115	-1.6747	-0.1036837	-11.92362131	
5	93	2.0933	-0.4990802	-46.41445854	-5	92	-2.0933	-0.4990802	-45.91537834	
6	73	2.512	-0.8082674	-59.00352219	-6	72	-2.512	-0.8082674	-58.19525476	
7	54	2.9307	-0.9778375	-52.80322307	-7	47	-2.9307	-0.9778375	-45.95836082	
8	34	3.3493	-0.9784994	-33.26897946	-8	37	-3.3493	-0.9784994	-36.20447764	
9	13	3.768	-0.8101389	-10.53180547	-9	18	-3.768	-0.8101389	-14.58249988	
10	7	4.1867	-0.5018379	-3.512865365	-10	3	-4.1867	-0.5018379	-1.505513728	
				304.2850396					101.6062684	

at (t=5)

x	h(x)	(2πxt)/60	cos(2πxt)/60	h(x)cos(2πxt)/60	x	h(x)	(2πxt)/60	cos(2πxt)/60	h(x)cos(2πxt)/60	Hr(t)
0	200	0	1	200						13.8855
1	185	0.5233	0.8661581	160.2392475	-1	180	-0.5233	0.8661581	155.908457	
2	164	1.0467	0.5004597	82.075389	-2	161	-1.0467	0.5004597	80.57400993	
3	140	1.57	0.0007963	0.11148574	-3	141	-1.57	0.0007963	0.112282066	
4	119	2.0933	-0.4990802	-59.39054372	-4	115	-2.0933	-0.4990802	-57.39422293	
5	93	2.6167	-0.865361	-80.47857631	-5	92	-2.6167	-0.865361	-79.61321527	
6	73	3.14	-0.9999987	-72.99990742	-6	72	-3.14	-0.9999987	-71.99990868	
7	54	3.6633	-0.866953	-46.81545963	-7	47	-3.6633	-0.866953	-40.74678894	
8	34	4.1867	-0.5018379	-17.06248891	-8	37	-4.1867	-0.5018379	-18.56800264	
9	13	4.71	-0.002389	-0.031056715	-9	18	-4.71	-0.002389	-0.043001606	
10	7	5.2333	0.4976994	3.483896106	-10	3	-5.2333	0.4976994	1.493098331	
				169.1319856					-30.27729275	

at (t=6)

x	h(x)	(2πxt)/60	cos(2πxt)/60	h(x)cos(2πxt)/60	x	h(x)	(2πxt)/60	cos(2πxt)/60	h(x)cos(2πxt)/60	Hr(t)
0	200	0	1	200						4.31745
1	185	0.628	0.8092042	149.7027735	-1	180	-0.628	0.8092042	145.6567526	
2	164	1.256	0.3096228	50.77814134	-2	161	-1.256	0.3096228	49.8492729	
3	140	1.884	-0.308108	-43.13512438	-3	141	-1.884	-0.308108	-43.44323241	
4	119	2.512	-0.8082674	-96.18382385	-4	115	-2.512	-0.8082674	-92.95075414	
5	93	3.14	-0.9999987	-92.99988205	-5	92	-3.14	-0.9999987	-91.99988332	
6	73	3.768	-0.8101389	-59.1401384	-6	72	-3.768	-0.8101389	-58.32999951	
7	54	4.396	-0.3111368	-16.80138771	-7	47	-4.396	-0.3111368	-14.62343004	
8	34	5.024	0.3065925	10.42414391	-8	37	-5.024	0.3065925	11.34392131	
9	13	5.652	0.8073286	10.4952721	-9	18	-5.652	0.8073286	14.53191522	
10	7	6.28	0.9999949	6.999964488	-10	3	-6.28	0.9999949	2.999984781	
				120.1399389					-76.96545263	

at (t=7)

x	h(x)	(2πxt)/60	cos(2πxt)/60	h(x)cos(2πxt)/60	x	h(x)	(2πxt)/60	cos(2πxt)/60	h(x)cos(2πxt)/60	Hr(t)
0	200	0	1	200						4.6484
1	185	0.7327	0.7433934	137.5277856	-1	180	-0.7327	0.7433934	133.8108185	
2	164	1.4653	0.1052676	17.26388659	-2	161	-1.4653	0.1052676	16.94808378	
3	140	2.198	-0.5868829	-82.16361279	-3	141	-2.198	-0.5868829	-82.75049574	
4	119	2.9307	-0.9778375	-116.3626583	-4	115	-2.9307	-0.9778375	-112.4513084	
5	93	3.6633	-0.866953	-80.62662493	-5	92	-3.6633	-0.866953	-79.75967197	
6	73	4.396	-0.3111368	-22.71298709	-6	72	-4.396	-0.3111368	-22.40185028	
7	54	5.1287	0.4043588	21.83537696	-7	47	-5.1287	0.4043588	19.00486513	
8	34	5.8613	0.9123322	31.01929525	-8	37	-5.8613	0.9123322	33.75629189	
9	13	6.594	0.9520847	12.37710142	-9	18	-6.594	0.9520847	17.13752505	
10	7	7.3267	0.5032149	3.522503996	-10	3	-7.3267	0.5032149	1.50964457	
				121.6800668					-75.19609751	

at (t=8)

x	h(x)	(2πxt)/60	cos(2πxt)/60	h(x)cos(2πxt)/60	x	h(x)	(2πxt)/60	cos(2πxt)/60	h(x)cos(2πxt)/60	Hr(t)
0	200	0	1	200						6.80086
1	185	0.8373	0.6694462	123.8475406	-1	180	-0.8373	0.6694462	120.5003097	
2	164	1.6747	-0.1036837	-17.00412083	-2	161	-1.6747	-0.1036837	-16.69306984	
3	140	2.512	-0.8082674	-113.1574398	-3	141	-2.512	-0.8082674	-113.9657072	
4	119	3.3493	-0.9784994	-116.4414281	-4	115	-3.3493	-0.9784994	-112.5274305	
5	93	4.1867	-0.5018379	-46.67092556	-5	92	-4.1867	-0.5018379	-46.16908765	
6	73	5.024	0.3065925	22.38125016	-6	72	-5.024	0.3065925	22.07465769	
7	54	5.8613	0.9123322	49.26593951	-7	47	-5.8613	0.9123322	42.87961402	
8	34	6.6987	0.9149221	31.1073526	-8	37	-6.6987	0.9149221	33.852119	
9	13	7.536	0.31265	4.064450217	-9	18	-7.536	0.31265	5.6277003	
10	7	8.3733	-0.4963174	-3.47422198	-10	3	-8.3733	-0.4963174	-1.488952277	
				133.9183968					-65.90984676	

a(t=9)

x	h(x)	(2πxt)/60	cos(2πxt)/60	h(x)cos(2πxt)/60	x	h(x)	(2πxt)/60	cos(2πxt)/60	h(x)cos(2πxt)/60	Hr(t)
0	200	0	1	200						6.47191
1	185	0.942	0.5881717	108.8117701	-1	180	-0.942	0.5881717	105.8709115	
2	164	1.884	-0.308108	-50.52971713	-2	161	-1.884	-0.308108	-49.60539304	
3	140	2.826	-0.9506126	-133.0857637	-3	141	-2.826	-0.9506126	-134.0363763	
4	119	3.768	-0.8101389	-96.40652697	-4	115	-3.768	-0.8101389	-93.16597144	
5	93	4.71	-0.002389	-0.222174964	-5	92	-4.71	-0.002389	-0.219785986	
6	73	5.652	0.8073286	58.9349895	-6	72	-5.652	0.8073286	58.12766088	
7	54	6.594	0.9520847	51.41257514	-7	47	-6.594	0.9520847	44.74798207	
8	34	7.536	0.31265	10.63010057	-8	37	-7.536	0.31265	11.56805062	
9	13	8.478	-0.5843009	-7.595911989	-9	18	-8.478	-0.5843009	-10.5174166	
10	7	9.42	-0.9999886	-6.999920099	-10	3	-9.42	-0.9999886	-2.999965757	
				134.9494204					-70.23030413	

at(t=10)

x	h(x)	(2πxt)/60	cos(2πxt)/60	h(x)cos(2πxt)/60	x	h(x)	(2πxt)/60	cos(2πxt)/60	h(x)cos(2πxt)/60	Hr(t)
0	200	0	1	200						3.86513
1	185	1.0467	0.5004597	92.58504247	-1	180	-1.0467	0.5004597	90.08274402	
2	164	2.0933	-0.4990802	-81.84915269	-2	161	-2.0933	-0.4990802	-80.3519121	
3	140	3.14	-0.9999987	-139.9998224	-3	141	-3.14	-0.9999987	-140.9998212	
4	119	4.1867	-0.5018379	-59.7187112	-4	115	-4.1867	-0.5018379	-57.71135956	
5	93	5.2333	0.4976994	46.28604827	-5	92	-5.2333	0.4976994	45.78834883	
6	73	6.28	0.9999949	72.99962966	-6	72	-6.28	0.9999949	71.99963474	
7	54	7.3267	0.5032149	27.17360225	-7	47	-7.3267	0.5032149	23.65109826	
8	34	8.3733	-0.4963174	-16.87479247	-8	37	-8.3733	-0.4963174	-18.36374475	
9	13	9.42	-0.9999886	-12.99985161	-9	18	-9.42	-0.9999886	-17.99979454	
10	7	10.467	-0.5045905	-3.532133691	-10	3	-10.467	-0.5045905	-1.513771582	
				124.0698585					-85.41857786	

Find a value (Hr) by applying the equation below to the tables.

Hr = 0.1∑ 60.

The values of Fourier transforms of the true sample Hr(t) obtained from table (3.4) as well as the values of Fourier transforms of the standard sample Gr(t) and Fourier transforms Fr(t) values calculated from equation (2.9) are included in the table(3.5).

Table (3.5):The values of Fourier transforms F(L), H(L) and G(L) for different values of (t) of the line (200).

t	Hr(t)	Gr(t)	Fr(t)
0	194.8	310	0.628387097
1	178.5383399	285	0.626450315
2	136.4207732	221.9451137	0.614659953
3	84.7213454	147.1725846	0.575659833
4	40.5891308	86.61593449	0.468610436
5	13.88546928	51.508148	0.269578112
6	4.317448632	36.65179608	0.117796373
7	4.648396928	29.42099292	0.157995923
8	6.800855001	20.94081616	0.324765518
9	6.47191163	10.76566563	0.601162237
10	3.865128068	3.274671358	1.180310219
			0.556537601

Other peaks such as peaks(220),(311) and (222) have been calculated as the integrated intensity profile function for the crystals h(x) values of figures (3.3), (3.4) and (3.5) respectively, and the values of Fourier transforms of the true sample Hr(t) calculate for the peak (220) and listed in table (3.6) ,and for the peak (311) are listed in table (3.7), and for the peak (222) are listed in table (3.8).

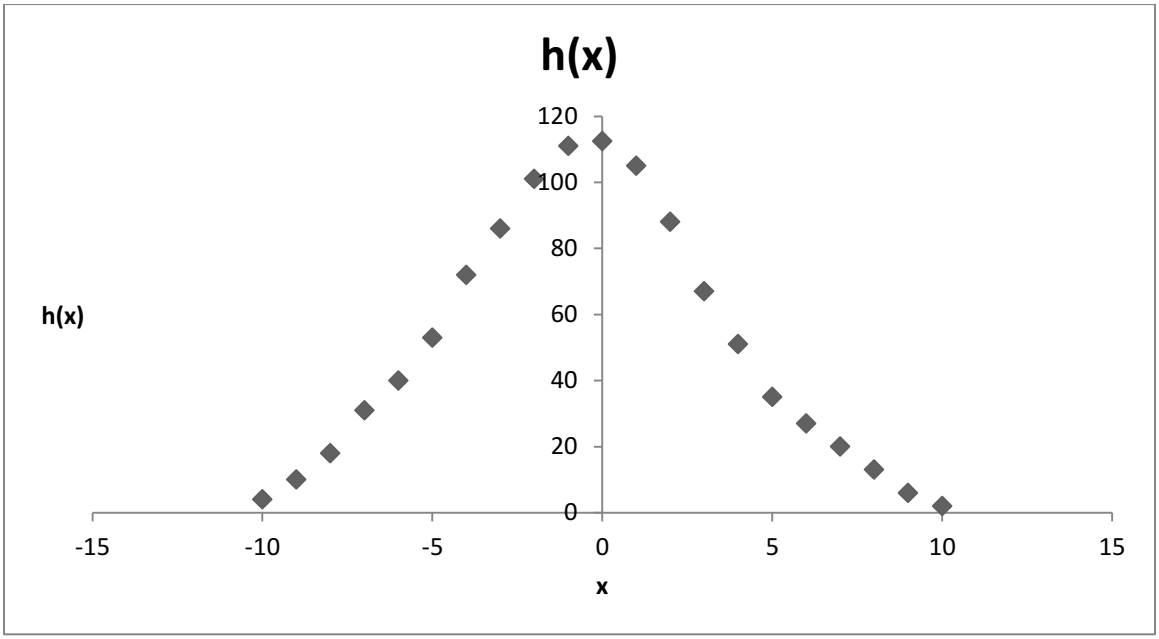

Figure (3.3) : h(x) highs as a function of the distance x of the peak (220).

Table (3.6) : The values of the integrated intensity profile function for the crystals h(x) for (220) peak and (x) and Fourier transforms of the true sample Hr(t) at all values of periodic time t from 0 to 10.

at (t=0)

x	h(x)	(2πxt)/60	cos(2πxt)/60	h(x)cos(2πxt)/60	x	h(x)	(2πxt)/60	cos(2πxt)/60	h(x)cos(2πxt)/60	Hr(t)
0	112.5	0	1	112.5						105.3
1	105	0	1	105	-1	111	0	1	111	
2	88	0	1	88	-2	101	0	1	101	
3	67	0	1	67	-3	86	0	1	86	
4	51	0	1	51	-4	72	0	1	72	
5	35	0	1	35	-5	53	0	1	53	
6	27	0	1	27	-6	40	0	1	40	
7	20	0	1	20	-7	31	0	1	31	
8	13	0	1	13	-8	18	0	1	18	
9	6	0	1	6	-9	10	0	1	10	
10	2	0	1	2	-10	4	0	1	4	
				526.5					526	

at (t=1)

x	h(x)	(2πxt)/60	cos(2πxt)/60	h(x)cos(2πxt)/60	x	h(x)	(2πxt)/60	cos(2πxt)/60	h(x)cos(2πxt)/60	Hr(t)
0	112.5	0	1	112.5						97.16
1	105	0.104667	0.994527443	104.4253815	-1	111	-0.10467	0.99452744	110.3925462	
2	88	0.209333	0.978169671	86.07893102	-2	101	-0.20933	0.97816967	98.79513673	
3	67	0.314	0.95110572	63.72408324	-3	86	-0.314	0.95110572	81.79509191	
4	51	0.418667	0.913631809	46.59522227	-4	72	-0.41867	0.91363181	65.78149026	
5	35	0.523333	0.866158094	30.3155333	-5	53	-0.52333	0.86615809	45.906379	
6	27	0.628	0.809204181	21.84851289	-6	40	-0.628	0.80920418	32.36816724	
7	20	0.732667	0.743393436	14.86786872	-7	31	-0.73267	0.74339344	23.04519651	
8	13	0.837333	0.669446165	8.702800149	-8	18	-0.83733	0.66944617	12.05003097	
9	6	0.942	0.58817173	3.529030382	-9	10	-0.942	0.58817173	5.881717303	
10	2	1.046667	0.500459689	1.000919378	-10	4	-1.04667	0.50045969	2.001838756	
				493.5882829					478.0175949	

at (t=2)

x	h(x)	(2πxt)/60	cos(2πxt)/60	h(x)cos(2πxt)/60	x	h(x)	(2πxt)/60	cos(2πxt)/60	h(x)cos(2πxt)/60	Hr(t)
0	112.5	0	1	112.5						76.16
1	105	0.209333	0.978169671	102.7078154	-1	111	-0.20933	0.97816967	108.5768334	
2	88	0.418667	0.913631809	80.3995992	-2	101	-0.41867	0.91363181	92.27681272	
3	67	0.628	0.809204181	54.21668013	-3	86	-0.628	0.80920418	69.59155956	
4	51	0.837333	0.669446165	34.14175443	-4	72	-0.83733	0.66944617	48.2001239	
5	35	1.046667	0.500459689	17.51608912	-5	53	-1.04667	0.50045969	26.52436352	
6	27	1.256	0.309622813	8.359815953	-6	40	-1.256	0.30962281	12.38491252	
7	20	1.465333	0.105267601	2.105352023	-7	31	-1.46533	0.1052676	3.263295635	
8	13	1.674667	-0.10368366	-1.347887627	-8	18	-1.67467	-0.10368366	-1.866305945	
9	6	1.884	-0.30810803	-1.848648188	-9	10	-1.884	-0.30810803	-3.081080313	
10	2	2.093333	-0.4990802	-0.998160399	-10	4	-2.09333	-0.4990802	-1.996320797	
				407.7524101					353.8741942	

at (t=3)

x	h(x)	(2πxt)/60	cos(2πxt)/60	h(x)cos(2πxt)/60	x	h(x)	(2πxt)/60	cos(2πxt)/60	h(x)cos(2πxt)/60	Hr(t)
0	112.5	0	1	112.5						50.22
1	105	0.314	0.95110572	99.86610059	-1	111	-0.314	0.95110572	105.5727349	
2	88	0.628	0.809204181	71.20996793	-2	101	-0.628	0.80920418	81.72962228	
3	67	0.942	0.58817173	39.40750593	-3	86	-0.942	0.58817173	50.58276881	
4	51	1.256	0.309622813	15.79076347	-4	72	-1.256	0.30962281	22.29284254	
5	35	1.57	0.000796327	0.027871435	-5	53	-1.57	0.00079633	0.042205316	
6	27	1.884	-0.30810803	-8.318916845	-6	40	-1.884	-0.30810803	-12.32432125	
7	20	2.198	-0.58688295	-11.73765897	-7	31	-2.198	-0.58688295	-18.1933714	
8	13	2.512	-0.80826743	-10.50747655	-8	18	-2.512	-0.80826743	-14.54881369	
9	6	2.826	-0.9506126	-5.703675589	-9	10	-2.826	-0.9506126	-9.506125981	
10	2	3.14	-0.99999873	-1.999997463	-10	4	-3.14	-0.99999873	-3.999994927	
				300.5344839					201.6475466	

at (t=4)

x	h(x)	(2πxt)/60	cos(2πxt)/60	h(x)cos(2πxt)/60	x	h(x)	(2πxt)/60	cos(2πxt)/60	h(x)cos(2πxt)/60	Hr(t)
0	112.5	0	1	112.5						27.67
1	105	0.418667	0.913631809	95.93133996	-1	111	-0.41867	0.91363181	101.4131308	
2	88	0.837333	0.669446165	58.91126254	-2	101	-0.83733	0.66944617	67.61406269	
3	67	1.256	0.309622813	20.74472847	-3	86	-1.256	0.30962281	26.62756192	
4	51	1.674667	-0.10368366	-5.287866843	-4	72	-1.67467	-0.10368366	-7.465223779	
5	35	2.093333	-0.4990802	-17.46780698	-5	53	-2.09333	-0.4990802	-26.45125057	
6	27	2.512	-0.80826743	-21.82322054	-6	40	-2.512	-0.80826743	-32.33069709	
7	20	2.930667	-0.97783746	-19.55674929	-7	31	-2.93067	-0.97783746	-30.31296139	
8	13	3.349333	-0.9784994	-12.72049215	-8	18	-3.34933	-0.9784994	-17.61298912	
9	6	3.768	-0.81013888	-4.860833293	-9	10	-3.768	-0.81013888	-8.101388821	
10	2	4.186667	-0.50183791	-1.003675818	-10	4	-4.18667	-0.50183791	-2.007351637	
				205.3666861					71.37289302	

at (t=5)

x	h(x)	(2πxt)/60	cos(2πxt)/60	h(x)cos(2πxt)/60	x	h(x)	(2πxt)/60	cos(2πxt)/60	h(x)cos(2πxt)/60	Hr(t)
0	112.5	0	1	112.5						13.29
1	105	0.523333	0.866158094	90.94659991	-1	111	-0.52333	0.86615809	96.14354848	
2	88	1.046667	0.500459689	44.04045263	-2	101	-1.04667	0.50045969	50.54642859	
3	67	1.57	0.000796327	0.05335389	-3	86	-1.57	0.00079633	0.068484097	
4	51	2.093333	-0.4990802	-25.45309017	-4	72	-2.09333	-0.4990802	-35.93377435	
5	35	2.616667	-0.86536104	-30.28763624	-5	53	-2.61667	-0.86536104	-45.86413489	
6	27	3.14	-0.99999873	-26.99996576	-6	40	-3.14	-0.99999873	-39.99994927	
7	20	3.663333	-0.86695296	-17.33905912	-7	31	-3.66333	-0.86695296	-26.87554164	
8	13	4.186667	-0.50183791	-6.52389282	-8	18	-4.18667	-0.50183791	-9.033082366	
9	6	4.71	-0.00238898	-0.014333869	-9	10	-4.71	-0.00238898	-0.023889781	
10	2	5.233333	0.497699444	0.995398888	-10	4	-5.23333	0.49769944	1.990797775	
				141.9178273					-8.981113356	

at (t=6)

x	h(x)	(2πxt)/60	cos(2πxt)/60	h(x)cos(2πxt)/60	x	h(x)	(2πxt)/60	cos(2πxt)/60	h(x)cos(2πxt)/60	Hr(t)
0	112.5	0	1	112.5						6.952
1	105	0.628	0.809204181	84.966439	-1	111	-0.628	0.80920418	89.82166409	
2	88	1.256	0.309622813	27.24680755	-2	101	-1.256	0.30962281	31.27190412	
3	67	1.884	-0.30810803	-20.6432381	-3	86	-1.884	-0.30810803	-26.49729069	
4	51	2.512	-0.80826743	-41.22163879	-4	72	-2.512	-0.80826743	-58.19525476	
5	35	3.14	-0.99999873	-34.99995561	-5	53	-3.14	-0.99999873	-52.99993278	
6	27	3.768	-0.81013888	-21.87374982	-6	40	-3.768	-0.81013888	-32.40555528	
7	20	4.396	-0.31113681	-6.222736189	-7	31	-4.396	-0.31113681	-9.645241093	
8	13	5.024	0.306592468	3.985702084	-8	18	-5.024	0.30659247	5.518664423	
9	6	5.652	0.807328623	4.84397174	-9	10	-5.652	0.80732862	8.073286233	
10	2	6.28	0.999994927	1.999989854	-10	4	-6.28	0.99999493	3.999979708	
				110.5815917					-41.05777604	

at (t=7)

x	h(x)	(2πxt)/60	cos(2πxt)/60	h(x)cos(2πxt)/60	x	h(x)	(2πxt)/60	cos(2πxt)/60	h(x)cos(2πxt)/60	Hr(t)
0	112.5	0	1	112.5						5.292
1	105	0.732667	0.743393436	78.05631077	-1	111	-0.73267	0.74339344	82.51667139	
2	88	1.465333	0.105267601	9.2635489	-2	101	-1.46533	0.1052676	10.63202771	
3	67	2.198	-0.58688295	-39.32115755	-3	86	-2.198	-0.58688295	-50.47193357	
4	51	2.930667	-0.97783746	-49.86971068	-4	72	-2.93067	-0.97783746	-70.40429743	
5	35	3.663333	-0.86695296	-30.34335347	-5	53	-3.66333	-0.86695296	-45.94850668	
6	27	4.396	-0.31113681	-8.400693856	-6	40	-4.396	-0.31113681	-12.44547238	
7	20	5.128667	0.404358833	8.087176651	-7	31	-5.12867	0.40435883	12.53512381	
8	13	5.861333	0.912332213	11.86031877	-8	18	-5.86133	0.91233221	16.42197984	
9	6	6.594	0.952084725	5.712508349	-9	10	-6.594	0.95208472	9.520847248	
10	2	7.326667	0.503214857	1.006429713	-10	4	-7.32667	0.50321486	2.012859426	
				98.5513776					-45.63070064	

at (t =8)

x	h(x)	(2πxt)/60	cos(2πxt)/60	h(x)cos(2πxt)/60	x	h(x)	(2πxt)/60	cos(2πxt)/60	h(x)cos(2πxt)/60	Hr(t)
0	112.5	0	1	112.5						4.678
1	105	0.837333	0.669446165	70.29184735	-1	111	-0.83733	0.66944617	74.30852435	
2	88	1.674667	-0.10368366	-9.124162397	-2	101	-1.67467	-0.10368366	-10.47205002	
3	67	2.512	-0.80826743	-54.15391763	-3	86	-2.512	-0.80826743	-69.51099875	
4	51	3.349333	-0.9784994	-49.90346919	-4	72	-3.34933	-0.9784994	-70.4519565	
5	35	4.186667	-0.50183791	-17.56432682	-5	53	-4.18667	-0.50183791	-26.59740919	
6	27	5.024	0.306592468	8.277996635	-6	40	-5.024	0.30659247	12.26369872	
7	20	5.861333	0.912332213	18.24664426	-7	31	-5.86133	0.91233221	28.28229861	
8	13	6.698667	0.914922135	11.89398776	-8	18	-6.69867	0.91492214	16.46859843	
9	6	7.536	0.312650017	1.8759001	-9	10	-7.536	0.31265002	3.126500167	
10	2	8.373333	-0.49631743	-0.992634851	-10	4	-8.37333	-0.49631743	-1.985269703	
				91.34786523					-44.56806389	

at (t=9)

x	h(x)	(2πxt)/60	cos(2πxt)/60	h(x)cos(2πxt)/60	x	h(x)	(2πxt)/60	cos(2πxt)/60	h(x)cos(2πxt)/60	Hr(t)
0	112.5	0	1	112.5						3.3
1	105	0.942	0.58817173	61.75803168	-1	111	-0.942	0.58817173	65.28706207	
2	88	1.884	-0.30810803	-27.11350675	-2	101	-1.884	-0.30810803	-31.11891116	
3	67	2.826	-0.9506126	-63.69104407	-3	86	-2.826	-0.9506126	-81.75268344	
4	51	3.768	-0.81013888	-41.31708299	-4	72	-3.768	-0.81013888	-58.32999951	
5	35	4.71	-0.00238898	-0.083614234	-5	53	-4.71	-0.00238898	-0.12661584	
6	27	5.652	0.807328623	21.79787283	-6	40	-5.652	0.80732862	32.29314493	
7	20	6.594	0.952084725	19.0416945	-7	31	-6.594	0.95208472	29.51462647	
8	13	7.536	0.312650017	4.064450217	-8	18	-7.536	0.31265002	5.6277003	
9	6	8.478	-0.58430092	-3.505805533	-9	10	-8.478	-0.58430092	-5.843009222	
10	2	9.42	-0.99998859	-1.999977171	-10	4	-9.42	-0.99998859	-3.999954342	
				81.45101848					-48.44863974	

at(t=10)

x	h(x)	(2πxt)/60	cos(2πxt)/60	h(x)cos(2πxt)/60	x	h(x)	(2πxt)/60	cos(2πxt)/60	h(x)cos(2πxt)/60	Hr(t)
0	112.5	0	1	112.5						1.36
1	105	1.046667	0.500459689	52.54826735	-1	111	-1.04667	0.50045969	55.55102548	
2	88	2.093333	-0.4990802	-43.91905754	-2	101	-2.09333	-0.4990802	-50.40710013	
3	67	3.14	-0.99999873	-66.99991503	-3	86	-3.14	-0.99999873	-85.99989093	
4	51	4.186667	-0.50183791	-25.59373337	-4	72	-4.18667	-0.50183791	-36.13232946	
5	35	5.233333	0.497699444	17.41948053	-5	53	-5.23333	0.49769944	26.37807052	
6	27	6.28	0.999994927	26.99986303	-6	40	-6.28	0.99999493	39.99979708	
7	20	7.326667	0.503214857	10.06429713	-7	31	-7.32667	0.50321486	15.59966055	
8	13	8.373333	-0.49631743	-6.452126535	-8	18	-8.37333	-0.49631743	-8.933713663	
9	6	9.42	-0.99998859	-5.999931513	-9	10	-9.42	-0.99998859	-9.999885856	
10	2	10.46667	-0.50459053	-1.009181055	-10	4	-10.4667	-0.50459053	-2.018362109	
				69.55796299					-55.96272853	

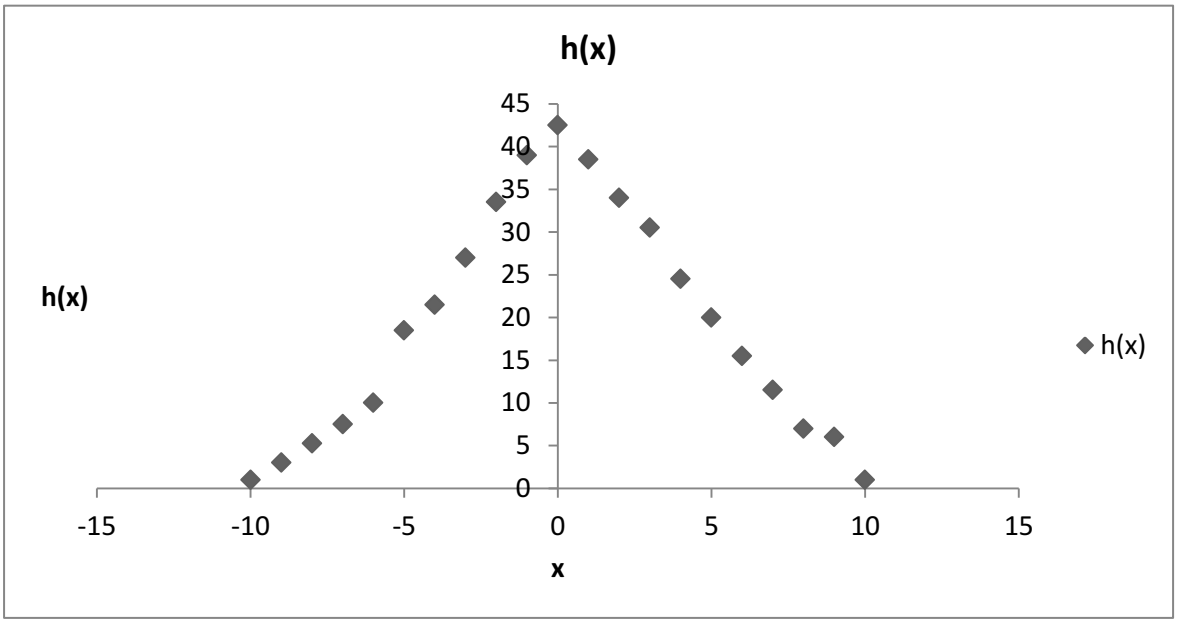

Figure (3.4) : h(x) highs as a function of the distance x of the peak (311).

Table (3.7): The values of the integrated intensity profile function for the crystals h(x) for (331) peak and (x) and Fourier transforms of the true sample Hr(t) at all values of periodic time t from 0 to 10.

at (t =0)

x	h(x)	(2πxt)/60	cos(2πxt)/60	h(x)cos(2πxt)/60	x	h(x)	(2πxt)/60	cos(2πxt)/60	h(x)cos(2πxt)/60	Hr(t)
0	43	0	1	42.5						39.725
1	39	0	1	38.5	-1	39	0	1	39	
2	34	0	1	34	-2	34	0	1	33.5	
3	31	0	1	30.5	-3	27	0	1	27	
4	25	0	1	24.5	-4	22	0	1	21.5	
5	20	0	1	20	-5	19	0	1	18.5	
6	16	0	1	15.5	-6	10	0	1	10	
7	12	0	1	11.5	-7	7.5	0	1	7.5	
8	7	0	1	7	-8	5.3	0	1	5.25	
9	6	0	1	6	-9	3	0	1	3	
10	1	0	1	1	-10	1	0	1	1	
				231					166.25	

at (t=1)

x	h(x)	(2πxt)/60	cos(2πxt)/60	h(x)cos(2πxt)/60	x	h(x)	(2πxt)/60	cos(2πxt)/60	h(x)cos(2πxt)/60	Hr(t)
0	43	0	1	42.5						36.492
1	39	0.10467	0.99452744	38.28930656	-1	39	-0.1047	0.99452744	38.78657029	
2	34	0.20933	0.97816967	33.2577688	-2	34	-0.2093	0.97816967	32.76868397	
3	31	0.314	0.95110572	29.00872446	-3	27	-0.314	0.95110572	25.67985444	
4	25	0.41867	0.91363181	22.38397932	-4	22	-0.4187	0.91363181	19.6430839	
5	20	0.52333	0.86615809	17.32316189	-5	19	-0.5233	0.86615809	16.02392475	
6	16	0.628	0.80920418	12.54266481	-6	10	-0.628	0.80920418	8.09204181	
7	12	0.73267	0.74339344	8.549024513	-7	7.5	-0.7327	0.74339344	5.575450769	
8	7	0.83733	0.66944617	4.686123157	-8	5.3	-0.8373	0.66944617	3.514592368	
9	6	0.942	0.58817173	3.529030382	-9	3	-0.942	0.58817173	1.764515191	
10	1	1.04667	0.50045969	0.500459689	-10	1	-1.0467	0.50045969	0.500459689	
				212.5702436					152.3491772	

at(t=2)

x	h(x)	(2πxt)/60	cos(2πxt)/60	h(x)cos(2πxt)/60	x	h(x)	(2πxt)/60	cos(2πxt)/60	h(x)cos(2πxt)/60	Hr(t)
0	43	0	1	42.5						28.1424
1	39	0.20933	0.97816967	37.65953232	-1	39	-0.2093	0.97816967	38.14861715	
2	34	0.41867	0.91363181	31.06348151	-2	34	-0.4187	0.91363181	30.60666561	
3	31	0.628	0.80920418	24.68072752	-3	27	-0.628	0.80920418	21.84851289	
4	25	0.83733	0.66944617	16.40143105	-4	22	-0.8373	0.66944617	14.39309255	
5	20	1.04667	0.50045969	10.00919378	-5	19	-1.0467	0.50045969	9.258504247	
6	16	1.256	0.30962281	4.799153602	-6	10	-1.256	0.30962281	3.096228131	
7	12	1.46533	0.1052676	1.210577413	-7	7.5	-1.4653	0.1052676	0.789507008	
8	7	1.67467	-0.1036837	-0.725785645	-8	5.3	-1.6747	-0.1036837	-0.544339234	
9	6	1.884	-0.308108	-1.848648188	-9	3	-1.884	-0.308108	-0.924324094	
10	1	2.09333	-0.4990802	-0.499080199	-10	1	-2.0933	-0.4990802	-0.499080199	
	231	0		165.2505832		166			116.1733841	

at(t=3)

x	h(x)	(2πxt)/60	cos(2πxt)/60	h(x)cos(2πxt)/60	x	h(x)	(2πxt)/60	cos(2πxt)/60	h(x)cos(2πxt)/60	Hr(t)
0	43	0	1	42.5						17.946
1	39	0.314	0.95110572	36.61757022	-1	39	-0.314	0.95110572	37.09312308	
2	34	0.628	0.80920418	27.51294215	-2	34	-0.628	0.80920418	27.10834006	
3	31	0.942	0.58817173	17.93923778	-3	27	-0.942	0.58817173	15.88063672	
4	25	1.256	0.30962281	7.58575892	-4	22	-1.256	0.30962281	6.656890481	
5	20	1.57	0.00079633	0.015926534	-5	19	-1.57	0.00079633	0.014732044	
6	16	1.884	-0.308108	-4.775674485	-6	10	-1.884	-0.308108	-3.081080313	
7	12	2.198	-0.5868829	-6.749153908	-7	7.5	-2.198	-0.5868829	-4.401622114	
8	7	2.512	-0.8082674	-5.657871991	-8	5.3	-2.512	-0.8082674	-4.243403993	
9	6	2.826	-0.9506126	-5.703675589	-9	3	-2.826	-0.9506126	-2.851837794	
10	1	3.14	-0.9999987	-0.999998732	-10	1	-3.14	-0.9999987	-0.999998732	
				108.2850609					71.17577944	

at (t=4)

x	h(x)	(2πxt)/60	cos(2πxt)/60	h(x)cos(2πxt)/60	x	h(x)	(2πxt)/60	cos(2πxt)/60	h(x)cos(2πxt)/60	Hr(t)
0	43	0	1	42.5						9.2842
1	39	0.41867	0.91363181	35.17482465	-1	39	-0.4187	0.91363181	35.63164056	
2	34	0.83733	0.66944617	22.76116962	-2	34	-0.8373	0.66944617	22.42644654	
3	31	1.256	0.30962281	9.443495798	-3	27	-1.256	0.30962281	8.359815953	
4	25	1.67467	-0.1036837	-2.540249758	-4	22	-1.6747	-0.1036837	-2.229198767	
5	20	2.09333	-0.4990802	-9.981603987	-5	19	-2.0933	-0.4990802	-9.232983688	
6	16	2.512	-0.8082674	-12.52814512	-6	10	-2.512	-0.8082674	-8.082674273	
7	12	2.93067	-0.9778375	-11.24513084	-7	7.5	-2.9307	-0.9778375	-7.333780982	
8	7	3.34933	-0.9784994	-6.849495771	-8	5.3	-3.3493	-0.9784994	-5.137121828	
9	6	3.768	-0.8101389	-4.860833293	-9	3	-3.768	-0.8101389	-2.430416646	
10	1	4.18667	-0.5018379	-0.501837909	-10	1	-4.1867	-0.5018379	-0.501837909	
				61.37219339					31.46988895	

at (t=5)

x	h(x)	(2πxt)/60	cos(2πxt)/60	h(x)cos(2πxt)/60	x	h(x)	(2πxt)/60	cos(2πxt)/60	h(x)cos(2πxt)/60	Hr(t)
0	43	0	1	42.5						4.0034
1	39	0.52333	0.86615809	33.34708663	-1	39	-0.5233	0.86615809	33.78016568	
2	34	1.04667	0.50045969	17.01562943	-2	34	-1.0467	0.50045969	16.76539958	
3	31	1.57	0.00079633	0.024287965	-3	27	-1.57	0.00079633	0.021500821	
4	25	2.09333	-0.4990802	-12.22746488	-4	22	-2.0933	-0.4990802	-10.73022429	
5	20	2.61667	-0.865361	-17.30722071	-5	19	-2.6167	-0.865361	-16.00917916	
6	16	3.14	-0.9999987	-15.49998034	-6	10	-3.14	-0.9999987	-9.999987317	
7	12	3.66333	-0.866953	-9.969958996	-7	7.5	-3.6633	-0.866953	-6.502147171	
8	7	4.18667	-0.5018379	-3.512865365	-8	5.3	-4.1867	-0.5018379	-2.634649023	
9	6	4.71	-0.002389	-0.014333869	-9	3	-4.71	-0.002389	-0.007166934	
10	1	5.23333	0.49769944	0.497699444	-10	1	-5.2333	0.49769944	0.497699444	
				34.8528793					5.181411638	

at (t=6)

x	h(x)	(2πxt)/60	cos(2πxt)/60	h(x)cos(2πxt)/60	x	h(x)	(2πxt)/60	cos(2πxt)/60	h(x)cos(2πxt)/60	Hr(t)
0	43	0	1	42.5						1.917
1	39	0.628	0.80920418	31.15436097	-1	39	-0.628	0.80920418	31.55896306	
2	34	1.256	0.30962281	10.52717564	-2	34	-1.256	0.30962281	10.37236424	
3	31	1.884	-0.308108	-9.397294954	-3	27	-1.884	-0.308108	-8.318916845	
4	25	2.512	-0.8082674	-19.80255197	-4	22	-2.512	-0.8082674	-17.37774969	
5	20	3.14	-0.9999987	-19.99997463	-5	19	-3.14	-0.9999987	-18.49997654	
6	16	3.768	-0.8101389	-12.55715267	-6	10	-3.768	-0.8101389	-8.101388821	
7	12	4.396	-0.3111368	-3.578073309	-7	7.5	-4.396	-0.3111368	-2.333526071	
8	7	5.024	0.30659247	2.146147276	-8	5.3	-5.024	0.30659247	1.609610457	
9	6	5.652	0.80732862	4.84397174	-9	3	-5.652	0.80732862	2.42198587	
10	1	6.28	0.99999493	0.999994927	-10	1	-6.28	0.99999493	0.999994927	
				26.83660302					-7.66863941	

at (t=7)

x	h(x)	(2πxt)/60	cos(2πxt)/60	h(x)cos(2πxt)/60	x	h(x)	(2πxt)/60	cos(2πxt)/60	h(x)cos(2πxt)/60	Hr(t)
0	43	0	1	42.5						1.561
1	39	0.73267	0.74339344	28.62064728	-1	39	-0.7327	0.74339344	28.992344	
2	34	1.46533	0.1052676	3.579098439	-2	34	-1.4653	0.1052676	3.526464638	
3	31	2.198	-0.5868829	-17.89992993	-3	27	-2.198	-0.5868829	-15.84583961	
4	25	2.93067	-0.9778375	-23.95701788	-4	22	-2.9307	-0.9778375	-21.02350548	
5	20	3.66333	-0.866953	-17.33905912	-5	19	-3.6633	-0.866953	-16.03862969	
6	16	4.396	-0.3111368	-4.822620547	-6	10	-4.396	-0.3111368	-3.111368095	
7	12	5.12867	0.40435883	4.650126574	-7	7.5	-5.1287	0.40435883	3.032691244	
8	7	5.86133	0.91233221	6.386325492	-8	5.3	-5.8613	0.91233221	4.789744119	
9	6	6.594	0.95208472	5.712508349	-9	3	-6.594	0.95208472	2.856254174	
10	1	7.32667	0.50321486	0.503214857	-10	1	-7.3267	0.50321486	0.503214857	
				27.93329352					-12.31862984	

at (t=8)

x	h(x)	(2πxt)/60	cos(2πxt)/60	h(x)cos(2πxt)/60	x	h(x)	(2πxt)/60	cos(2πxt)/60	h(x)cos(2πxt)/60	Hr(t)
0	43	0	1	42.5						1.476
1	39	0.83733	0.66944617	25.77367736	-1	39	-0.8373	0.66944617	26.10840045	
2	34	1.67467	-0.1036837	-3.525244562	-2	34	-1.6747	-0.1036837	-3.473402731	
3	31	2.512	-0.8082674	-24.65215653	-3	27	-2.512	-0.8082674	-21.82322054	
4	25	3.34933	-0.9784994	-23.9732352	-4	22	-3.3493	-0.9784994	-21.03773701	
5	20	4.18667	-0.5018379	-10.03675818	-5	19	-4.1867	-0.5018379	-9.284001321	
6	16	5.024	0.30659247	4.752183254	-6	10	-5.024	0.30659247	3.06592468	
7	12	5.86133	0.91233221	10.49182045	-7	7.5	-5.8613	0.91233221	6.842491599	
8	7	6.69867	0.91492214	6.404454946	-8	5.3	-6.6987	0.91492214	4.80334121	
9	6	7.536	0.31265002	1.8759001	-9	3	-7.536	0.31265002	0.93795005	
10	1	8.37333	-0.4963174	-0.496317426	-10	1	-8.3733	-0.4963174	-0.496317426	
				29.11432421					-14.35657104	

at (t=9)

x	h(x)	(2πxt)/60	cos(2πxt)/60	h(x)cos(2πxt)/60	x	h(x)	(2πxt)/60	cos(2πxt)/60	h(x)cos(2πxt)/60	Hr(t)
0	43	0	1	42.5						1.052
1	39	0.942	0.58817173	22.64461162	-1	39	-0.942	0.58817173	22.93869748	
2	34	1.884	-0.308108	-10.47567306	-2	34	-1.884	-0.308108	-10.32161905	
3	31	2.826	-0.9506126	-28.99368424	-3	27	-2.826	-0.9506126	-25.66654015	
4	25	3.768	-0.8101389	-19.84840261	-4	22	-3.768	-0.8101389	-17.41798597	
5	20	4.71	-0.002389	-0.047779562	-5	19	-4.71	-0.002389	-0.044196095	
6	16	5.652	0.80732862	12.51359366	-6	10	-5.652	0.80732862	8.073286233	
7	12	6.594	0.95208472	10.94897434	-7	7.5	-6.594	0.95208472	7.140635436	
8	7	7.536	0.31265002	2.188550117	-8	5.3	-7.536	0.31265002	1.641412587	
9	6	8.478	-0.5843009	-3.505805533	-9	3	-8.478	-0.5843009	-1.752902767	
10	1	9.42	-0.9999886	-0.999988586	-10	1	-9.42	-0.9999886	-0.999988586	
				26.92439613					-16.40920087	

at (t=10)

x	h(x)	(2πxt)/60	cos(2πxt)/60	h(x)cos(2πxt)/60	x	h(x)	(2πxt)/60	cos(2πxt)/60	h(x)cos(2πxt)/60	Hr(t)
0	43	0	1	42.5						0.5147
1	39	1.04667	0.50045969	19.26769803	-1	39	-1.0467	0.50045969	19.51792787	
2	34	2.09333	-0.4990802	-16.96872678	-2	34	-2.0933	-0.4990802	-16.71918668	
3	31	3.14	-0.9999987	-30.49996132	-3	27	-3.14	-0.9999987	-26.99996576	
4	25	4.18667	-0.5018379	-12.29502878	-4	22	-4.1867	-0.5018379	-10.78951505	
5	20	5.23333	0.49769944	9.953988875	-5	19	-5.2333	0.49769944	9.20743971	
6	16	6.28	0.99999493	15.49992137	-6	10	-6.28	0.99999493	9.999949269	
7	12	7.32667	0.50321486	5.78697085	-7	7.5	-7.3267	0.50321486	3.774111424	
8	7	8.37333	-0.4963174	-3.47422198	-8	5.3	-8.3733	-0.4963174	-2.605666485	
9	6	9.42	-0.9999886	-5.999931513	-9	3	-9.42	-0.9999886	-2.999965757	
10	1	10.4667	-0.5045905	-0.504590527	-10	1	-10.467	-0.5045905	-0.504590527	
				23.26611823					-18.11946198	

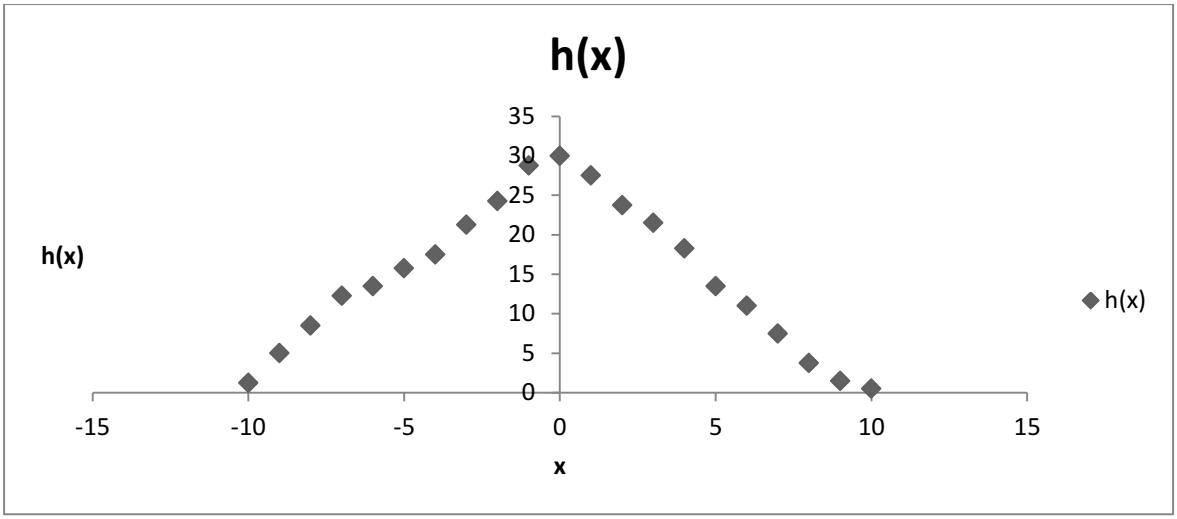

Figure (3.5) : h(x) highs as a function of the distance x of the peak (222).

Table (3.8) : the values of the integrated intensity profile function for the crystals h(x) for (222) peak and (x) and Fourier transforms of the true sample Hr(t) at all values of periodic time t from 0 to 10.

at (t=0)

x	h(x)	(2πxt)/60	cos(2πxt)/60	h(x)cos(2πxt)/60	x	h(x)	(2πxt)/60	cos(2πxt)/60	h(x)cos(2πxt)/60	Hr(t)
0	30	0	1	30						31
1	28	0	1	27.5	-1	29	0	1	28.75	
2	24	0	1	23.75	-2	24	0	1	24.25	
3	22	0	1	21.5	-3	21	0	1	21.25	
4	18	0	1	18.25	-4	18	0	1	17.5	
5	14	0	1	13.5	-5	16	0	1	15.75	
6	11	0	1	11	-6	14	0	1	13.5	
7	7.5	0	1	7.5	-7	12	0	1	12.25	
8	3.8	0	1	3.75	-8	8.5	0	1	8.5	
9	1.5	0	1	1.5	-9	5	0	1	5	
10	0.5	0	1	0.5	-10	1.3	0	1	1.25	
	159			158.75		148			148	

at (t=1)

x	h(x)	(2πxt)/60	cos(2πxt)/60	h(x)cos(2πxt)/60	x	h(x)	(2πxt)/60	cos(2πxt)/60	h(x)cos(2πxt)/60	Hr(t)
0	30	0	1	30						27.9
1	28	0.10467	0.9945274	27.34950469	-1	28.8	-0.10467	0.99452744	28.59266399	
2	24	0.20933	0.9781697	23.23152968	-2	24.3	-0.20933	0.97816967	23.72061451	
3	22	0.314	0.9511057	20.44877298	-3	21.3	-0.314	0.95110572	20.21099655	
4	18	0.41867	0.9136318	16.67378052	-4	17.5	-0.41867	0.91363181	15.98855666	
5	14	0.52333	0.8661581	11.69313427	-5	15.8	-0.52333	0.86615809	13.64198999	
6	11	0.628	0.8092042	8.901245991	-6	13.5	-0.628	0.80920418	10.92425644	
7	7.5	0.73267	0.7433934	5.575450769	-7	12.3	-0.73267	0.74339344	9.10656959	
8	3.8	0.83733	0.6694462	2.51042312	-8	8.5	-0.83733	0.66944617	5.690292405	
9	1.5	0.942	0.5881717	0.882257595	-9	5	-0.942	0.58817173	2.940858652	
10	0.5	1.04667	0.5004597	0.250229845	-10	1.25	-1.04667	0.50045969	0.625574611	
	159			147.5163295		148			131.4423734	

at(t=2)

x	h(x)	(2πxt)/60	cos(2πxt)/60	h(x)cos(2πxt)/60	x	h(x)	(2πxt)/60	cos(2πxt)/60	h(x)cos(2πxt)/60	Hr(t)
0	30	0	1	30						21
1	28	0.2093	0.97817	26.89966594	-1	29	-0.2093	0.97817	28.12237803	
2	24	0.4187	0.913632	21.69875547	-2	24	-0.4187	0.913632	22.15557137	
3	22	0.628	0.809204	17.39788989	-3	21	-0.628	0.809204	17.19558885	
4	18	0.8373	0.669446	12.21739252	-4	18	-0.8373	0.669446	11.71530789	
5	14	1.0467	0.50046	6.756205802	-5	16	-1.0467	0.50046	7.882240102	
6	11	1.256	0.309623	3.405850944	-6	14	-1.256	0.309623	4.179907976	
7	7.5	1.4653	0.105268	0.789507008	-7	12	-1.4653	0.105268	1.289528114	
8	3.8	1.6747	-0.103684	-0.388813738	-8	8.5	-1.6747	-0.103684	-0.881311141	
9	1.5	1.884	-0.308108	-0.462162047	-9	5	-1.884	-0.308108	-1.540540156	
10	0.5	2.0933	-0.49908	-0.2495401	-10	1.3	-2.0933	-0.49908	-0.623850249	
	159			118.0647517		148			89.49482079	

at (t=3)

x	h(x)	(2πxt)/60	cos(2πxt)/60	h(x)cos(2πxt)/60	x	h(x)	(2πxt)/60	cos(2πxt)/60	h(x)cos(2πxt)/60	Hr(t)
0	30	0	1	30						12
1	28	0.314	0.951106	26.1554073	-1	29	-0.314	0.951106	27.34428945	
2	24	0.628	0.809204	19.2185993	-2	24	-0.628	0.809204	19.62320139	
3	22	0.942	0.588172	12.6456922	-3	21	-0.942	0.588172	12.49864927	
4	18	1.256	0.309623	5.650616338	-4	18	-1.256	0.309623	5.418399228	
5	14	1.57	0.000796	0.010750411	-5	16	-1.57	0.000796	0.012542146	
6	11	1.884	-0.308108	-3.389188344	-6	14	-1.884	-0.308108	-4.159458422	
7	7.5	2.198	-0.586883	-4.401622114	-7	12	-2.198	-0.586883	-7.189316119	
8	3.8	2.512	-0.808267	-3.031002852	-8	8.5	-2.512	-0.808267	-6.870273132	
9	1.5	2.826	-0.950613	-1.425918897	-9	5	-2.826	-0.950613	-4.753062991	
10	0.5	3.14	-0.999999	-0.499999366	-10	1.3	-3.14	-0.999999	-1.249998415	
	159			80.93333397		148			40.6749724	

at (t=4)

x	h(x)	(2πxt)/60	cos(2πxt)/60	h(x)cos(2πxt)/60	x	h(x)	(2πxt)/60	cos(2πxt)/60	h(x)cos(2πxt)/60	Hr(t)
0	30	0	1	30						5.12
1	28	0.4187	0.913632	25.12487475	-1	29	-0.4187	0.913632	26.26691451	
2	24	0.8373	0.669446	15.89934643	-2	24	-0.8373	0.669446	16.23406951	
3	22	1.256	0.309623	6.656890481	-3	21	-1.256	0.309623	6.579484777	
4	18	1.6747	-0.103684	-1.892226861	-4	18	-1.6747	-0.103684	-1.814464113	
5	14	2.0933	-0.49908	-6.737582691	-5	16	-2.0933	-0.49908	-7.86051314	
6	11	2.512	-0.808267	-8.8909417	-6	14	-2.512	-0.808267	-10.91161027	
7	7.5	2.9307	-0.977837	-7.333780982	-7	12	-2.9307	-0.977837	-11.97850894	
8	3.8	3.3493	-0.978499	-3.669372734	-8	8.5	-3.3493	-0.978499	-8.317244864	
9	1.5	3.768	-0.810139	-1.215208323	-9	5	-3.768	-0.810139	-4.050694411	
10	0.5	4.1867	-0.501838	-0.250918955	-10	1.3	-4.1867	-0.501838	-0.627297387	
	159			47.69107941		148			3.520135677	

at(t =5)

x	h(x)	(2πxt)/60	cos(2πxt)/60	h(x)cos(2πxt)/60	x	h(x)	(2πxt)/60	cos(2πxt)/60	h(x)cos(2πxt)/60	Hr(t)
0	30	0	1	30						1.3
1	28	0.5233	0.866158	23.8193476	-1	29	-0.5233	0.866158	24.90204521	
2	24	1.0467	0.50046	11.88591761	-2	24	-1.0467	0.50046	12.13614746	
3	22	1.57	0.000796	0.017121024	-3	21	-1.57	0.000796	0.016921943	
4	18	2.0933	-0.49908	-9.108213638	-4	18	-2.0933	-0.49908	-8.733903489	
5	14	2.6167	-0.865361	-11.68237398	-5	16	-2.6167	-0.865361	-13.62943631	
6	11	3.14	-0.999999	-10.99998605	-6	14	-3.14	-0.999999	-13.49998288	
7	7.5	3.6633	-0.866953	-6.502147171	-7	12	-3.6633	-0.866953	-10.62017371	
8	3.8	4.1867	-0.501838	-1.88189216	-8	8.5	-4.1867	-0.501838	-4.265622228	
9	1.5	4.71	-0.002389	-0.003583467	-9	5	-4.71	-0.002389	-0.011944891	
10	0.5	5.2333	0.497699	0.248849722	-10	1.3	-5.2333	0.497699	0.622124305	
	159			25.79303949		148			-13.08382459	

at (t=6)

x	h(x)	(2πxt)/60	cos(2πxt)/60	h(x)cos(2πxt)/60	x	h(x)	(2πxt)/60	cos(2πxt)/60	h(x)cos(2πxt)/60	Hr(t)
0	30	0	1	30						0.382
1	27.5	0.628	0.80920418	22.25311498	-1	28.75	-0.628	0.809204181	23.2646202	
2	23.75	1.256	0.30962281	7.35354181	-2	24.25	-1.256	0.309622813	7.508353217	
3	21.5	1.884	-0.30810803	-6.624322672	-3	21.25	-1.884	-0.308108031	-6.547295665	
4	18.25	2.512	-0.80826743	-14.75088055	-4	17.5	-2.512	-0.808267427	-14.14467998	
5	13.5	3.14	-0.99999873	-13.49998288	-5	15.75	-3.14	-0.999998732	-15.74998002	
6	11	3.768	-0.81013888	-8.911527703	-6	13.5	-3.768	-0.810138882	-10.93687491	
7	7.5	4.396	-0.31113681	-2.333526071	-7	12.25	-4.396	-0.311136809	-3.811425916	
8	3.75	5.024	0.30659247	1.149721755	-8	8.5	-5.024	0.306592468	2.606035978	
9	1.5	5.652	0.80732862	1.210992935	-9	5	-5.652	0.807328623	4.036643117	
10	0.5	6.28	0.99999493	0.499997463	-10	1.25	-6.28	0.999994927	1.249993659	
				16.34712907					-12.52461032	

at (t=7)

x	h(x)	(2πxt)/60	cos(2πxt)/60	h(x)cos(2πxt)/60	x	h(x)	(2πxt)/60	cos(2πxt)/60	h(x)cos(2πxt)/60	Hr(t)
0	30	0	1	30						1
1	28	0.7327	0.743393	20.44331949	-1	29	-0.7327	0.743393	21.37256128	
2	24	1.4653	0.105268	2.500105527	-2	24	-1.4653	0.105268	2.552739327	
3	22	2.198	-0.586883	-12.61798339	-3	21	-2.198	-0.586883	-12.47126266	
4	18	2.9307	-0.977837	-17.84553372	-4	18	-2.9307	-0.977837	-17.11215563	
5	14	3.6633	-0.866953	-11.70386491	-5	16	-3.6633	-0.866953	-13.65450906	
6	11	4.396	-0.311137	-3.422504904	-6	14	-4.396	-0.311137	-4.200346928	
7	7.5	5.1287	0.404359	3.032691244	-7	12	-5.1287	0.404359	4.953395699	
8	3.8	5.8613	0.912332	3.421245799	-8	8.5	-5.8613	0.912332	7.754823812	
9	1.5	6.594	0.952085	1.428127087	-9	5	-6.594	0.952085	4.760423624	
10	0.5	7.3267	0.503215	0.251607428	-10	1.3	-7.3267	0.503215	0.629018571	
	159			15.48720964		148			-5.415311954	

at (t=8)

x	h(x)	(2πxt)/60	cos(2πxt)/60	h(x)cos(2πxt)/60	x	h(x)	(2πxt)/60	cos(2πxt)/60	h(x)cos(2πxt)/60	Hr(t)
0	30	0	1	30						1.6
1	28	0.8373	0.669446	18.40976955	-1	29	-0.8373	0.669446	19.24657725	
2	24	1.6747	-0.103684	-2.46248701	-2	24	-1.6747	-0.103684	-2.514328842	
3	22	2.512	-0.808267	-17.37774969	-3	21	-2.512	-0.808267	-17.17568283	
4	18	3.3493	-0.978499	-17.85761397	-4	18	-3.3493	-0.978499	-17.12373943	
5	14	4.1867	-0.501838	-6.774811775	-5	16	-4.1867	-0.501838	-7.90394707	
6	11	5.024	0.306592	3.372517148	-6	14	-5.024	0.306592	4.138998318	
7	7.5	5.8613	0.912332	6.842491599	-7	12	-5.8613	0.912332	11.17606961	
8	3.8	6.6987	0.914922	3.430958007	-8	8.5	-6.6987	0.914922	7.776838149	
9	1.5	7.536	0.31265	0.468975025	-9	5	-7.536	0.31265	1.563250083	
10	0.5	8.3733	-0.496317	-0.248158713	-10	1.3	-8.3733	-0.496317	-0.620396782	
	159			17.80389017		148			-1.436361538	

at (t=9)

x	h(x)	(2πxt)/60	cos(2πxt)/60	h(x)cos(2πxt)/60	x	h(x)	(2πxt)/60	cos(2πxt)/60	h(x)cos(2πxt)/60	Hr(t)
0	30	0	1	30						1.5
1	28	0.942	0.588172	16.17472258	-1	29	-0.942	0.588172	16.90993725	
2	24	1.884	-0.308108	-7.317565743	-2	24	-1.884	-0.308108	-7.471619758	
3	22	2.826	-0.950613	-20.43817086	-3	21	-2.826	-0.950613	-20.20051771	
4	18	3.768	-0.810139	-14.7850346	-4	18	-3.768	-0.810139	-14.17743044	
5	14	4.71	-0.002389	-0.032251205	-5	16	-4.71	-0.002389	-0.037626405	
6	11	5.652	0.807329	8.880614857	-6	14	-5.652	0.807329	10.89893642	
7	7.5	6.594	0.952085	7.140635436	-7	12	-6.594	0.952085	11.66303788	
8	3.8	7.536	0.31265	1.172437562	-8	8.5	-7.536	0.31265	2.657525142	
9	1.5	8.478	-0.584301	-0.876451383	-9	5	-8.478	-0.584301	-2.921504611	
10	0.5	9.42	-0.999989	-0.499994293	-10	1.3	-9.42	-0.999989	-1.249985732	
	159			19.41894236		148			-3.929247971	

at (t=10)

x	h(x)	2πxt)/60	cos(2πxt)/60	h(x)cos(2πxt)/60	x	h(x)	(2πxt)/60	cos(2πxt)/60	h(x)cos(2πxt)/60	Hr(t)
0	30	0	1	30						0.9
1	28	1.0467	0.50046	13.76264145	-1	29	-1.047	0.50046	14.38821606	
2	24	2.0933	-0.49908	-11.85315473	-2	24	-2.093	-0.49908	-12.10269483	
3	22	3.14	-0.999999	-21.49997273	-3	21	-3.14	-1	-21.24997305	
4	18	4.1867	-0.501838	-9.158541843	-4	18	-4.187	-0.50184	-8.782163411	
5	14	5.2333	0.497699	6.718942491	-5	16	-5.233	0.497699	7.838766239	
6	11	6.28	0.999995	10.9999442	-6	14	-6.28	0.999995	13.49993151	
7	7.5	7.3267	0.503215	3.774111424	-7	12	-7.327	0.503215	6.164381992	
8	3.8	8.3733	-0.496317	-1.861190347	-8	8.5	-8.373	-0.49632	-4.218698119	
9	1.5	9.42	-0.999989	-1.499982878	-9	5	-9.42	-0.99999	-4.999942928	
10	0.5	10.467	-0.504591	-0.252295264	-10	1.3	-10.47	-0.50459	-0.630738159	
				19.13050176					-10.0929147	

Find a value (Hr) by applying the equation below to the tables.

$$Hr = 0.1\sum h(x)\cos(2\pi xt)/60$$

Then the values of Fourier transforms of the true sample Hr(t) from the Tables (3.6) , (3.7) and (3.8) are listed in the Tables (3.9), (3.10) and (3.11) respectively also listed the values of Fourier transforms of the standard sample Gr(t) and Fourier transforms Fr(t) for the peaks (22o) ,(311) and (222) .

Table (3.9): The values of Fourier transforms F(L), H(L) and G(L) for different values of (t) of the peak (220).

t	Hr(t)	Gr(t)	Fr(t)
0	105.25	310	0.339516129
1	97.16058778	285	0.340914343
2	76.16266043	221.9451137	0.343159888
3	50.21820305	147.1725846	0.341219822
4	27.67395791	86.61593449	0.319501926
5	13.2936714	51.508148	0.258088709
6	6.952381569	36.65179608	0.189687336
7	5.292067696	29.42099292	0.179873865
8	4.677980134	20.94081616	0.223390535
9	3.300237873	10.76566563	0.306552143
10	1.359523446	3.274671358	0.415163324
			0.325706802

Equation (2.9) was used to calculate the value Fourier transforms Fr(t) for each value of Fourier transforms of the true sample Hr(t) and Fourier transforms of the standard sample Gr(t) , and the results were included in the table (3.9).

Table (3.10) :The values of Fourier transforms F(L), H(L) and G(L) for different values of (t) of peak(311).

t	Hr(t)	Gr(t)	Fr(t)
0	39.725	310	0.128145161
1	36.49194207	285	0.128041902
2	28.14239672	221.9451137	0.126798902
3	17.94608403	147.1725846	0.121939042
4	9.284208234	86.61593449	0.107188225
5	4.003429094	51.508148	0.07772419
6	1.916796361	36.65179608	0.052297474
7	1.561466367	29.42099292	0.053073204
8	1.475775317	20.94081616	0.070473629
9	1.051519526	10.76566563	0.097673434
10	0.514665625	3.274671358	0.157165581
			0.112052074

Equation (2.9) was used to calculate the value Fourier transforms Fr (t) for each value of Fourier transforms of the true sample Hr(t) and Fourier transforms of the standard sample Gr(t) , and the results were included in the table (3.10).

Table (3.11): The values of Fourier transforms F(L), H(L) and G(L) for different values of (t) of the peak (222).

t	Hr(t)	Gr(t)	Fr(t)
0	0.903	310	0.002912903
1	27.89587029	285	0.097880247
2	20.75595725	221.9451137	0.093518424
3	12.16083064	147.1725846	0.082629728
4	5.121121509	86.61593449	0.059124473
5	1.27092149	51.508148	0.024674183
6	0.382251875	36.65179608	0.010429281
7	1.007189769	29.42099292	0.034233711
8	1.636752863	20.94081616	0.078160892
9	1.548969439	10.76566563	0.143880508
10	0.903758706	3.274671358	0.275984551
			0.09034289

Equation (2.9) was used to calculate the value Fourier transforms Fr (t) for each value of Fourier transforms of the true sample Hr(t) and Fourier transforms of the standard sample Gr(t), and the results were included in the table(3.11).

After calculating $F_r(t)$from equation (2.10) to calculate the values $F_r(t)$. The average $F_r(t)$ values for each diffraction peak were taken then equations (2.11) and (2.12) were used to determine the particle size D and lattice strain $< \varepsilon^2 >$ respectively for the lines (111) , (200) . (220) , (311) and (222) and the results are set out in the table (3.12).

Table (3.12) : The crystallite size and lattice strain for the peaks (111), (200) ,(220) , (311) and (222) of the x- ray diffraction of Manganese oxide (MnO) nanoparticle.

Peak (hkl)	Diffraction angle 2θ degree	Reflection angle θ degree	inter planer spacing d nm	Fourier length L nm	crystallite size D nm	lattice strain $< \varepsilon^2 > \times 10^{-4}$
(111)	35.5	17.75	0.2527	6.162	5.3885	0.9699
(200)	40.6	20.3	0.222	9.427	16.087	0.1648
(220)	59	29.5	0.1564	10.162	9.0594	0.134
(311)	74.25	37.125	0.1276	8.854	3.6828	0.2583
(222)	70.75	35.375	0.133	8.753	3.9999	0.2562
					7.64352	0.35664

The table (3.12) shows that the crystallite size increases with the decrease of the lattice strain this result fails in some times because of extracting information regarding the size distribution and strain profile by analyzing the theta dependence of the cosine Fourier coefficients (which describes the symmetric broadening) . Therefore the disproportion between particle size and strain due to the some liens is not symmetric broadening .

3.2 Debye - Scherrer Method

In this method, equation (2.6) is used to calculate the particle size of each peak of diffraction peaks and β represents FWHM calculated in radians and the wavelength of the copper is used equal to λ= 0.15046 nm and listed d the result in Table (3.13). Also this table shows the values of strain which was calculated using the equation (2.7). In this method we can see that the inverse of the relation between the particle size and strain .

Table (3.13) : The particle size and strain calculation for the lines (111) , (200) , (220) , (311) and (222) by Debye – Scherrer method .

Peak	β (2θ) radian	θ degree	4tan(θ)	cos(θ)	particle size D nm	Strain $\varepsilon \times 10^{-4}$
(111)	0.02128	17.75	1.2804	0.95239	6.7647	166.2126
(200)	0.01788	20.3	1.47964	0.93788	8.1731	120.8398
(220)	0.01808	29.5	2.26308	0.87142	8.7094	79.930608
(311)	0.02289	35.375	2.84002	0.81538	7.3445	80.6182
(222)	0.02253	37.125	3.02792	0.75698	7.6324	74.0752
					7.72482	104.33528

The breadth of the width of the peak indicates the large number of crystalline defects, leading to an increase in the value of the strain and therefore prefer less value for the strain and less FWHM (β(2θ)radian)to reduce the crystalline defects.

3.3 Williamson–Hall Method

The line diffraction profile was analyzed using Williamson–Hall technique ,we have used figure (3.6) to find FWHM (β_{hkl})and then we have find FWHM(β_{hkl}) and 2θ to determine the β_{hkl} cosθ and 4sinθ for each peak MnO nano particles, the results are listed in Table (3.14), the β_{hkl} cosθ is the y-axis and 4sinθ is the x-axis in Williamson –hall as shown in Figure (3.6). Williamson-Hall was used to find the size of the D crystals and the ε lattice strain using equation (2.14). Graph format, the crystallite size D is obtained from the y-intercept and the lattice strain ε *is* obtained from the slope .

Table (3-14): The values of β (2θ) cosθ and 4sinθ for the lines (111) , (200) , (220) , (311) and (222) by Williamson –Hall method of XRD pattern of MnO nanoparticles .

Peak	β(2θ)radian	θ degree	COS(θ)	β(2θ)COS(θ)	SIN(θ)	4SIN(θ)
(111)	0.02128	17.75	0.952395	0.0202688	0.304864	1.219456
(200)	0.01788	20.3	0.937888	0.016769	0.3469356	1.3877424
(220)	0.01808	29.5	0.870355	0.015736	0.4924235	1.969694
(311)	0.02289	35.375	0.81538	0.018668	0.578925	2.3157
(222)	0.01796	37.125	0.79732	0.017964	0.603555	2.41422

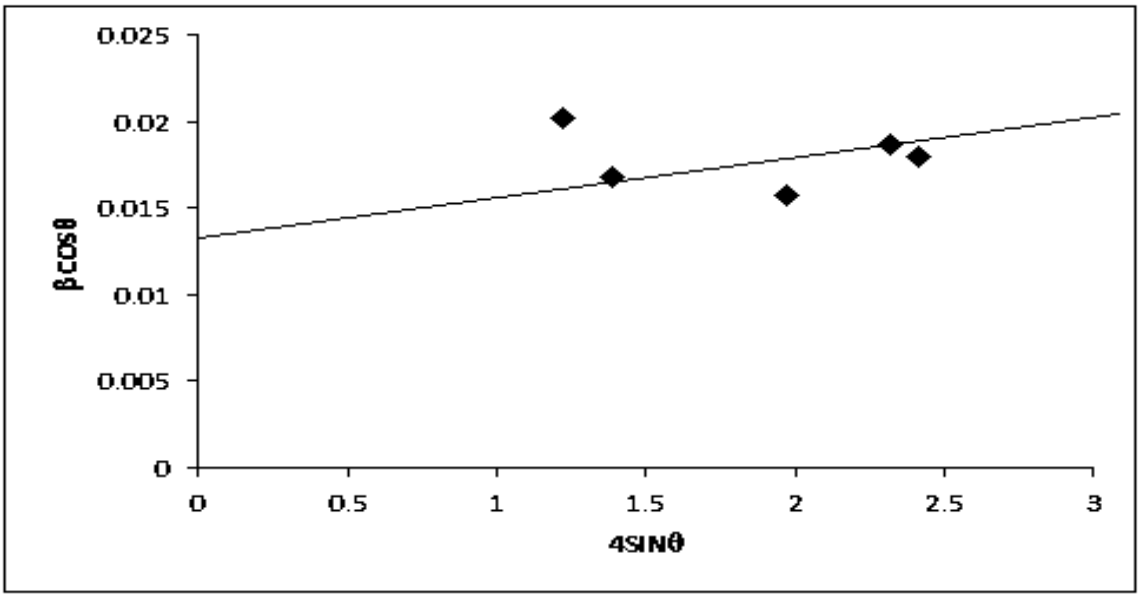

Figure (3.6): Williamson –hall plot of β_{hkl} cosθ ,4sinθ of MnO nanoparticles.

From the figure (3.6) we get :

$$intercept = \frac{k\lambda}{D}$$

$$D = \frac{k\lambda}{intercept}$$

D = 9.864 nm

As well from the slope which represents values ε strain :

ε = slope , then $\varepsilon = 20.833 \times 10^{-4}$

This method gives the results more accurate from Debye - Scherrer method because it used the straight line which gives the particle size (from the y-intercept) and the strain (from the slope) in one time .

3.4 Alteration Scherrer Method

In this method we used the calculate the ln1/cos(θ) and lnβ(2θ) for all peaks (111) , (200) , (220) , (311) and (222) as shown in table (3.15) ,we used the diagram to calculate the average particle size, equation (2.16) was used get a straight peak as shown in the figure (3.7) .

Table (3.15): The values of ln(1/cosθ) and values ln β of the peaks (111) , (200) , (220) , (311) and (222) for the Alteration Scherrer method.

peak	θ degree	cos(θ)	1/cos(θ)	ln1/cos(θ	β(2θ)radian	lnβ(2θ)
(111)	17.75	0.9524437	1.049931	0.0487243	0.02128	-3.89866
(200)	20.3	0.9379512	1.066154	0.0640573	0.01788	-4.0878
(220)	29.5	0.8704842	1.148786	0.1387057	0.01808	-4.0129
(311)	35.375	0.8155616	1.226149	0.2038783	0.02289	-3.9809
(222)	37.125	0.7975189	1.253889	0.2262498	0.01796	-4.01935

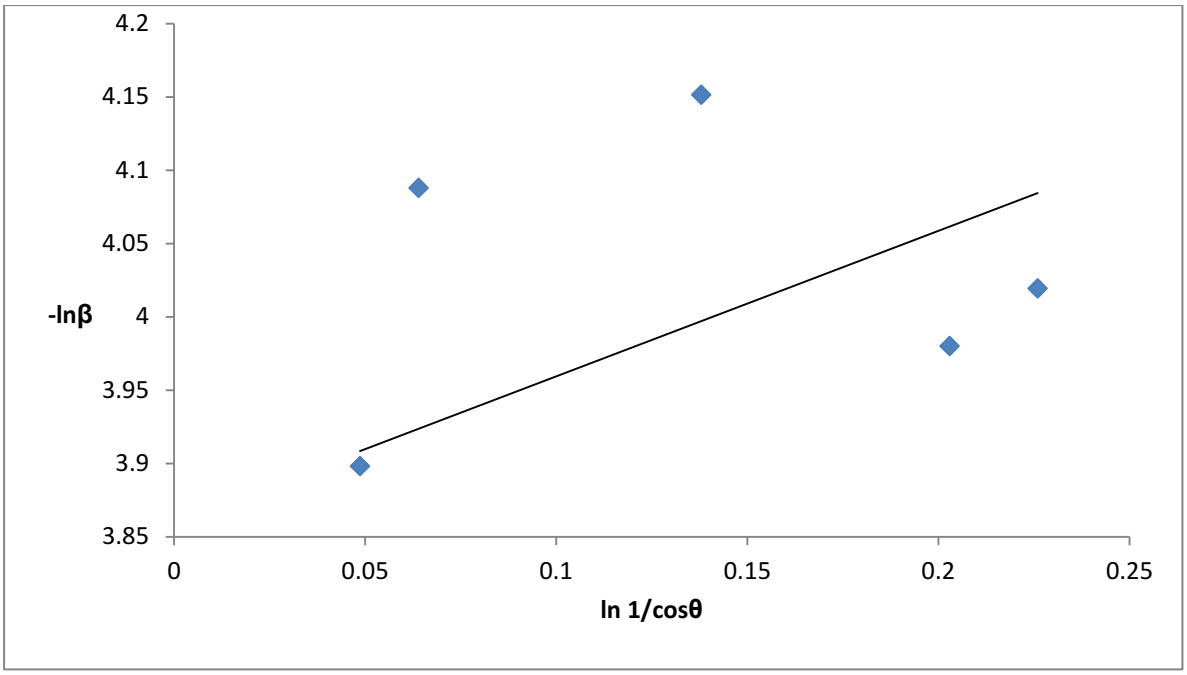

Figure (3.7) : The relation between the parameter of this method

And from intercept of Y- axis we can get on the particle size because the intercept equal to ln (k λ/D)

$$D = e^{\frac{k\lambda}{intercept}}$$

then:

D = 6.5081 nm

3.5 New Model in Strain of Alteration Scherrer Method

From the equation (2.24) the values of ln 4sinθ and ln $\beta cos\theta$ were calculated for each line in diffraction lines and the results were listed in table (3.16).

Table (3.16): The values of ln 4sinθ and ln $\beta cos\theta$ of the lines (111) , (200) , (220) , (311) and (222) for the new model of Alteration scherrer method.

Peak (hkl)	θ degree	sin(θ)	4sin(θ)	ln4sin(θ)	cos(θ)	$\beta(\theta)_{radian}$	lnβcos(θ)
(111)	17.75	0.304864	1.219456	0.198404	0.952395	0.021282	-3.898669
(200)	20.3	0.346935	1.38774	0.327675	0.937888	0.01788	-4.088197
(220)	29.5	0.492423	1.969692	0.677877	0.870355	0.01808	-4.01294
(311)	35.375	0.578925	2.3157	0.839712	0.81538	0.02289	-3.980937
(222)	37.125	0.603555	2.41422	0.881376	0.79732	0.02253	-4.019353

From the values of Table (3.16) drawing on figure (3.8) between the values of ln 4sinθ ,ln $\beta cos\theta$ of new- axis.

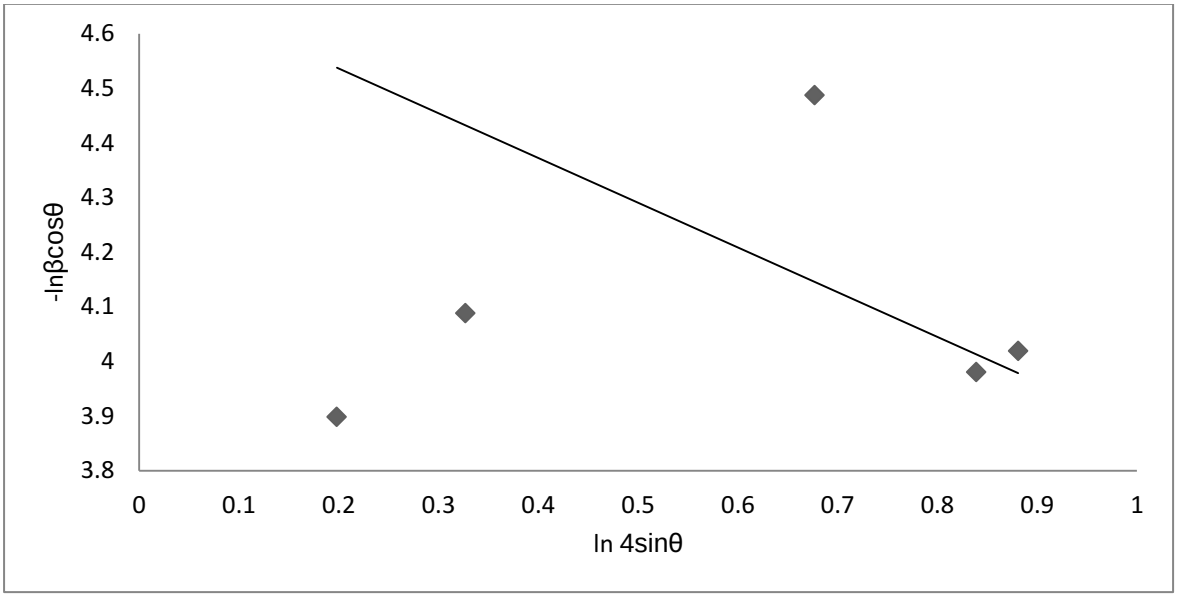

Figure(3.8): The relation between on the values of ln 4sinθ , ln $\beta cos\theta$ of new model of Alteration Scherrer method

And from this figure the strain was calculated as follows :

lnε = intercept

$\varepsilon = \quad 90 \times 10^{-4}$

Thus we can see the final results in Fourier analysis method and the other methods of analysis used in this work in table (3.17) .

Table (3.17): Measurements of crystallite size and lattice strain of the Fourier analysis method. Deby - Scherrer method. Williamson-hall method. New model and Modified scherrer method.

Fourier Analysis method		Debye -Sherrer method		Williamson–Hil method		Modifical Scherrer method	
D nm	$<\varepsilon^2>\times 10^{-4}$	D nm	$\varepsilon \times 10^{-4}$	D nm	$\varepsilon \times 10^{-4}$	D nm	$\varepsilon \times 10^{-4}$
7.6435	0.3566	8.4167	99.8351	9.8642	20.8333	6.5081	90

To comparing between the results of the Fourier method and other methods for analysis from the above table all three methods take the part of the area under the curve of the peaks but only Fourier analysis method take in the calculation all area under the curve ,this mean the Debye-Scherrer method dependent on FWHM and other three methods there for the results of the Fourier method to determine the particle size and strain is more accuracy from other method .

3.6 Parameters Calculation

1. Texture Coefficient (Tc)

Equation(2.18) was used to calculate the texture coefficient (T_c) for all lines of diffraction pattern and the results are listed in table (3.19). Shows the highs(Tc) value of t is for the (200) peak, meaning that level (200) has the best preferred orientation .

Table (3.18): Database Comments: Deleted Or Rejected By: Deleted by NBS card, 00-003-1145 (Fixed Slit Intensity) - Cu Kα1 1.54056A.

Type equation here. 2θ	d(l)	I	hkl	2θ	d(l)	hkl
36.1904	2.48	50		99.3974	1.01	80
41.3834	2.18	80	200	102.5991	0.987	100
59.5975	1.55	100	220	117.0841	0.903	100
71.4006	1.32	80	311	129.4005	0.852	80
74.6766	1.27	80	222	160.1358	0.782	60
88.8949	1.1	50	400			

Table (3.19): The values of texture coefficient (Tc) for peaks of diffraction peaks .

Peak (hkl)	TC
(111)	1.053169
(200)	2.044989
(220)	1.155419
(311)	0.439672
(222)	0.306748

The Texture Coefficient is used to describe the prevailing trend and represents the shape of the specified level, which includes a deviation from one. When Tc ≥1 is. This confirms that the direction of the crystal growth of the preferred levels is within this direction. When Tc≤1 is multi-crystallization, but in non-uniform directions, the improvement of crystalline growth of the material is associated with the value of this factor. If Tc = 1 is the ideal case for surface growth.

2. Micro Strain (S):

The micro strain was calculated using equation (2.19) then the results are listed in table (3.20). The micro strain depends directly on the $\beta(2\theta)$ and θis Bragg diffraction angle of the XRD peak . So the strain broadening is caused by varying displacement of the atoms with respect to their reference lattice position, recorded on the micro strain table (3.20).

Table (3.20): The values of micro strain for all the lines of diffraction pattern .

Peak (hkl)	θ degree	$\beta(2\theta)$ radian	$\beta(2\theta)\cos(\theta)$	Micro strain $< \varepsilon >$
(111)	17.75	0.021282	0.020268	5.067×10^{-3}
(200)	20.3	0.01788	0.016769	4.192×10^{-3}
(220)	29.5	0.018089	0.015743	3.935×10^{-3}
(311)	35.375	0.022895	0.018668	4.667×10^{-3}
(222)	37.125	0.022531	0.017964	4.491×10^{-3}

3. Dislocation density

To determine the dislocation density equation (2.20) was used and the values of dislocation density for all diffraction lines are listed in table (3.21) .The dislocation density decreases with the increase of the crystallites, where the crystallites size here represents crystallites calculated in the Fourier analysis method.

Table (3.21): The values of dislocation density for lines of diffraction peaks .

Peak (hkl)	D nm	Dislocation density (lines/m^2)
(111)	5.3885	34.4×10^{15}
(200)	16.087	3.8×10^{15}
(220)	9.0594	12.1×10^{15}
(311)	3.9999	62.5×10^{15}
(222)	3.6828	73.7×10^{15}

4. The Area of the Particle

Of equation (2.21) we can calculate the specific surface area of all diffraction peaks and the results listed in table (3.22). Where the results show that the relationship between the Area of the Particle and the particle size when increasing the size less the Area of the Particle. The value of the density ρ in equation (2.21) of MnO nano particle is equal to 5.39 gm/cm3 [67] .

Table (3.22): The values of the Area of the particle for lines of diffraction peaks .

Peak (hkl)	D nm	The Area of the particle (m^2/g)
(111)	5.3885	20.6583×10^4
(200)	16.087	6.9197×10^4
(220)	9.0594	12.2874×10^4
(311)	3.9999	27.8300×10^4
(222)	3.6828	30.2262×10^4

3.7 New Models

First New Model

Calculation between lattice strain and root mean strain of Fourier method I have been using equation (2.22) to find the value (ε)

$\varepsilon = 7.4828 \times 10^{-3}$

The result was equal and as shown in table (3.23).

Second New Model

The equation has been used (2.23) to find a value (u).

u = 2799614.7 dyne/cm^2

Intensity of the energy model and the result is also shown in table (3.23).

Third New Model

The equation (2.24) was used to find the stress which was based on the Young's modulus Y.

$\sigma = 7.4828 \times 10^{8}$ dyne $/cm^2$

The result is also shown in table (3.23).

Table(3.23): The calculated, stress and energy of MnO nanoparticles.

Strain (ε)	Stress (σ) dyne/ cm^2	Energy (u) dyne/ cm^2
7.4828×10^{-3}	7.4828×10^{8}	2799614.7

3.8 Size Broadening

Shows table (3.24) the relation between $< \varepsilon^2 >$,ε and μ .

Table(3. 24): The relation also between $< \varepsilon^2 >$, ε and μ .

strain coefficients		apparent strain
< ε2>	ε	μ
0.3566×10^{-4}	7.4828×10^{-3}	0.02993

Chapter Four
Conclusions and Recommendation

4.1 Conclusions

1- It can be measure the Crystallize sizes approximately 100 nm using powder diffraction method.

2- Using powder diffraction method it is possible to find vacancies, site disorder , dislocations that are formed by the presence of point defects such as vacancy, site disturbance, imbalances and even extended defects.

3- The Deby Shearer method does not give accuracy in the results because of the adoption of this method at the highest intensity without taking into account the intensity of integrated. This means that FWHM takes only part of the X-ray diffraction line area .

4- The Debye-Shearer equation can be developed in the computation of strain as a new model for the purpose of comparing results with other methods of analysis. Because Shearer gives a volume connector. In general, this method gives results different from the way of Debye - Shearer because it is used in calculating the average particle size and strain through the chart .

5- In the Williamson -Hull method, particle size and strain are calculated by the constructor diagram that links the two

6- Now that the Fourier method has been developed, it is possible to calculate the new properties of the crystalline structure such as the emotion plus the rate of the emotion box as well as the stress and energy. It is possible to develop this method to calculate other characteristics but they will be left at present as future work.

7- When comparing the Fourier method in the analysis of these methods which are used in this work. It was concluded that the results of the Fourier method are the most accurate results because this method is based mainly on the analysis of the X-ray diffraction line, starting from the line tails up to the top for the intensity and diffraction angle. Fourier methods are the most general method for extracting volume and intensity but require high accuracy in diffraction line analysis as well as in calculating granular size and emotion separately from each other.

8- The calculation of most of the crystalline parameters is linked to the particle size and the strain of the calculation. Therefore, the particle size must be calculated precisely because it gives accurate information about the crystalline structure .

4.2 Future work

1- Development of the Fourier method to determine some mechanical properties using x-ray diffraction technique .

2-The distinction between the Fourier method and the integrated intensity method, although both methods use integrated intensity.

3- using the diagram in the Fourier method to conduct a link between the particle size and the strain and then develop this method to calculate other properties of the crystalline structure.

4- A comparative study of the Fourier method and another important method is the method of variation to determine the accuracy of each method.

5- The use of mechanical tests of materials for comparison with the results obtained from X-ray diffraction lines using the Fourier method.

References

1. G. Ribárik, J. Gubicza, T. Ungár. “Correlation between strength and microstructure of ball-milled Al–Mg alloys determined by X-ray diffraction” Materials Science and Engineering. A 387–389,pp.343–347, (2004).
2. H. Chen, Y. L .Yao, J.Y. Wang . “ Fourier analysis of x-ray micro diffraction profiles to characterize laser shock peened metals ”. Vol .32,pp.506-518, (2004).
3. K. Kapoor , D. Lahiri , S .V vrrao, T. Sanyal and B. P kashyap , “ X-ray diffraction line profile analysis for defect study in Zr–2×5% Nb material ”, Indian Academy of Sciences, Vol . 27, No. 1,pp.59-67, (2004).
4. M. Meier , “ Crystallite size measurement using x-ray diffraction ”, University of California, Vol .13,(2004).
5. R .M .Stroud ,D. A. Agard , “ Structure determination of asymmetric membrane profiles using an iterative Fourier method ”, Biophysical Journal, Vol .25,No.3,pp495-512, (1979).
6. L. L. Thompson and P. M. Pinsky, “ Complex Wavenumber Fourier Analysis of P–Version finite element method”.Computational Mechanics,Vol.13,pp.255-275,(1994) .
7. S.G. Podorov1 , G. HoÈlzer , E. FoÈ rster , and N.N. Faleev , “ Fourier analysis of x-ray rocking curves from super lattices ” Phys .stat . sol,pp.213-317,(1999).
8. P Bala , B. K .Samantaray and S. K. Srivastava ,“ Dehydration transformation in Ca-montmorillonite”, Bulletin of Materials Science, Vol. 23, No. 1,pp.61-67,(2000).
9. B. Marinkovica , R. Ribeiro de Avilleza , A . Saavedrab , F. Cosme Rizzo Assunçãoa , “ Averbach method and alternate methods for x-ray diffraction microstructure analysis of polycrystalline specimen science”. Vol. 4, No. 2,pp.71-76, (2001).

10. J. M. Amigó , F. J.Serrano , M. A. Kojdecki , J. Bastida , V. Esteve , M. M. Reventós, and F. Martí , "X-ray diffraction microstructure analysis of mullite, quartz and corundum in porcelain insulators", Journal of the European Ceramic Society, Vol. 25, No. 9,pp.1479-1486, (2005).
11. M. S. Haluska , I. C. Dragomir , K. H. Sandhage , R. L and Snyder, "X-ray diffraction analyses of 3D MgO-based replicas of diatom micro shells synthesized by a low-temperature gas/solid displacement reaction", Journal of Materials characterization, Powder Diffraction, Vol. 20, No. 04,pp.306-310,(2005).
12. A. Milev , M. Wilson , G. S. K. Kannangara , and N.Tran , " X-ray diffraction line profile analysis of nano crystalline graphite", Materials Chemistry and Physics, Vol. 111, No. 2-3,pp.346-350, (2008).
13. V. I . Moni, J .T. Assis , S .A . Filippov , and S. M . lglesias., " Analysis of displacement and broadening of x-ray diffraction lines caused by surface stress gradient :computer simulation and measurement ", Rev . Adv . Mater Sci , Vol. 19 ,pp.166-171, (2009) .
14. R. Sen, S. Das and K. Das, "Microstructural Characterization of Nano sized Ceria Powders by X-Ray Diffraction Analysis", Metallurgical and Materials Transactions A, Vol. 42, No. 5,pp.1409-1417, (2011).
15. T . Many, K Thandavan , S. Meriam Abdul Gani , C . San Wong , R. Md Nor," Evaluation of Williamson–Hall strain and stress distribution in ZnO nanowires prepared using aliphatic alcohol ", J Non destruct Eval, Vol. 34, pp.14,(2015).
16. Dr.Ziad ,T. Khodair , A. H. Abed , S. G. Majeed ," Synthesis and Structural Characterization of MgO Nanoparticles ", International Journal of Advanced Research in Science , Engineering and Technology ,Vol. 3, No. 7 , (2016).

17. SH.Yadav ,M.Singh, D.K. Verma, J.Gantam, “X-Ray Diffraction Study of the Effects of Dopant on the Lattice Strain of Zinc Oxide Nanoparticles ”, Adv. Nano Energy, Vol.1,No.1,pp.73-89,(2017).
18. Y. Leng, “ Materials Characterization: Introduction to Microscopic and Spectroscopic Methods ”, Wiley publish, (2013).
19. B.D. Cullity, Elements of X Ray Diffraction.(2011): Biblio Bazaar.
20. R.M. Berman and I. Cohen, “Method for improve x-ray diffraction determinations of residual stress in nickel-base alloys”. (1990).
21. B .K .Pandey, A.K. Shahi, R. Gopal, “ Synthesis, optical properties and growth mechanism of MnO nano structures”. Applied Surface Science , Vol .283,pp.430-437, (2013).
22. P. Z. Si , H. X. Wang , W. Jiang, J. G. Lee, C. J. Choi and T. Sohnel, “Structure and magnetic properties of manganese oxide nanoparticles prepared by arc sublimation”, Modern Physics Letters B, Vol. 24, No. 31,pp.3025-3032, (2010).
23. A. Mishra, J. Dwivedi, K. Shukla, P. Malviya , “X-Ray diffraction and Fourier transformation infrared spectroscopy studies of copper (II) thiourea chloro andsulphate complexes ”, Journal of Physics: Conference Series ,Vol.534 **,** No.012014, (2014).
24. M.E .Fitzpatrickl , A. T.Fry ,P.Holdway, F.A.Kandil, J.Shackleton and L. Suominen,“Determination of residual stresses by x-ray diffraction” National Physical Laboratory ,Vol.2,No.52,(2005).
25. S. J. S. Qazi , A. R. Rennie , J. K. Cockcroft , M .Vickers , “Use of wide-angle X-ray diffraction to measure shape and size of dispersed Colloidal particles”,Journal of Colloid and Interface Science, Vol.338,No.1,pp.105-110, (2009) .
26. T.C. Huang and ,W. Parrish,“ Accurate and rapid reduction of experimental x-ray ”, Appl. Phys. Lett ,Vol. 27, pp.123-124,(1975).

27. M. K. Wu, J. R. Ashburn, C. J. Torng, P. H. Hor, R. L. Meng, L. Gao, Z. J. Hwang, Y. Q. Wang, and C. W. Chu, " Superconductivity at 93 K in a new mixed-phase Y-Ba-Cu-O compound system at ambient pressure" , Phys. Rev. Lett. Vol.58, No.908, (1987).
28. R. Delhez, T.H. Keijser, J. I. Langford, D. Louer, E.J. Mittemeijer, & E.J. Sonneveld , " Crystal imperfection broadening and peak shape in the Rietveld Method" . edited by R.A. Young, I U Cr Monograph #5, Oxford University Press, Ch. 8, (1993) .
29. S.A. Howard & DL Bish , "The Rietveld method and its pplications to synchrotron X-ray powder data ", Reviews in Mineralogy, Vol. 20, Mineralogical Society of America, Ch.8, (1989) .
30. P. Karen & P.M. Woodward, " Liquid-Mix Disorder in Crystalline Solids ScMnO " , J. Solid State Chem.Vol. 141, pp.78- 88, (1998).
31. N. Aldea, B. Barz, T. D. Silipas, F. Aldea, Z. Wu , " Mathematical study of metal nanoparticle size determination by single x-ray line Profile analysis ",Journal of Optoelectronics and Advanced Materials Vol. 7, No. 6,pp.3093-3100, (2005).
32. S. Vives , E. Gaffet , C. Meunier ,"X-ray diffraction line profile analysis of iron ball milled powders " Materials Science and Engineering ,Vol.366,pp.229-238, (2004).
33. J. Res," X-Ray diffraction line broadening: modeling and applications to high-Tc superconductors" , Journal of Research of the National Institute of Standards and Technology , Vol. 98, No. 3, (1993).
34. F. Raiteri, A. Senin, G. Fagherazzi , "An automatic system for X-ray diffraction line profile analysis", J. Mater. Science ,Vol.13, No.1717 ,(1978).

35. D. Taupin ,“Automatic peak determination in X-ray powder patterns ” , J. Appl. Cryst , Vol.6, No.266 ,(1973).
36. H. G. Riela , L . G. Martinez , K . Imakuma, “ Determination of crystallite size in UO_{2+x} , powder by x-ray diffraction ” , Journal of Nuclear Materials, Vol. 153,pp.71-75, (1988).
37. Sh. P. Dubeya , M. Lahtinenb , M. Sillanpääa , “ Tansy fruit mediated greener synthesis of silver and gold nanoparticles”,Process Biochemistry ,Vol.45,No.1,pp.1065-1071, (2010).
38. S.N. Anitha , I. Jayakumari ,“Synthesis and Analysis of Nano crystalline $Fe_2Mn_2Ni_{0.5}Zn_{1.5}O_9$ at Different Treating Temperatures ”, Journal of Nanoscience and Technology ,Vol. 1,No.2, pp.26-31,(2015).
39. M .J .Edoff , B. Kubler and PH. Thelin , “ Aa empirical scherrer equation for weakly swelling mixed –layer minerals , especially illite – smectite ”, Clay minerals,Vol.34,No.3,pp.601-617, (1999) .
40. A.S. de Menezes , C.M.R. Reme´dios , J.M. Sasaki , L.R.D. da Silva ,J.C. Goes , P.M. Jardim , M.A.R. Miranda , “ Sintering of oparticles of a-Fe2O3 using gelatin” , Journal of Non-Crystalline Solids ,Vol.353 ,pp.1091-1094,(2007).
41. M. JABOYEDOFF, B. KUBLER, “An empirical Scherrer equation swelling mixed-layer minerals, illite-smectite” , Clay Minerals Vol.34, ,pp.601-517,(1999).
42. R. Delhez , Th. H. de Keijser, and E. J. Mittemeijer, Fresenius Determination of crystallite size and lattice distortions through X-ray diffraction line profile analysis. Fresenius, Z. Anal. Chem. Vol,312,No. 1, (1982).
43. R Yogamalar , R Srinivasan , A Vinu , K Ariga , A. Ch Bose , “ X-ray peak broadening analysis in ZnO nanoparticles” ,Solid state communications ,Vol .149, pp1919–1923, (2009).

44. H . Sarma , K.C. Sarma , " X-Ray peak broadening analysis of ZnO nano particles derived by precipitation method ", International Journal of Scientific and Research Publications, Vol. 4, No. 3, pp. 2250-3153, (2014).
45. A. K. Zak , W.H. Abd. Majid , M.E. Abrishami , R. Yousefi , "X-ray analysis of ZnO nanoparticles by Williamson-Hall and size strain plot methods", Solid State Sciences ,Vol.13 ,pp.251-256,(2011).
46. T. M. K. Thandavan · S. M.A. Gani , " Evaluation of williamson–hall strain and stress distribution in ZnO nanowires prepared using aliphatic alcohol", J.Nondestruct Eval ,Vol.34, No.14 , (2015).
47. Y. T. Prabhu , K. V. Rao , V. S. Sai Kumar , B. S. Kumari , "X-Ray Analysis by Williamson-Hall and Size-Strain Plot Methods of ZnO Nanoparticles with Fuel Variation" , World Journal of Nano Science and Engineering, ,Vol.4,pp. 21-28,(2014) .
48. G. K. Williamson, W. H. Hall , " X-Ray line broadening from filed aluminium and wolfram" , Department of metallurgy, university of Birmingham, England. Acta Metall, Vol.1, pp.22–31,(1953).
49. Ch. Zhu, Lu. Bingan , Su. Qing , Xie .Erqing , and W. Lan , A simple method for the preparation of hollow ZnO nano spheres for use as a high performance photo catalyst, Cite this: Nanoscale, Vol.4, No.3060,(2012).
50. A. Monshi, M. R. Foroughi , M. R. Monshi , " Modified scherrer equation to estimate more accurately nano-crystallite size using xrd " World journal of nano science and engineering, Vol. 2, pp.154- 160, (2012).
51. Y. T. Prabhu, K. Venkateswara Methods Rao, V. Sesha Sai Kumar, B. Siva Kumari , " X-ray Analysis of Fe doped ZnO Nanoparticles by Williamson-Hall and Size-Strain Plot", International Journal of

Engineering and Advanced Technology , Vol.2, No.4, pp.2249 – 8958, (2013).

52. J. A. S. Salman , Z. A. Al-Ramadhan and H .A. Karem Hmud , " Antibacterial effect and structural properties of PVA-PVP-AG nanocomposites" . European Journal of Biomedical, Vol. 3, No.9, pp.35-41,(2016) .
53. A.V. Moholkar , S.S. Shinde , A.R. Babar , Kyu-Ung Sim , Ye-bin Kwon , K.Y. Rajpure , P.S. Patil , C.H. Bhosale , J.H. Kim, " Development of CZTS thin films solar cells by pulsed laser deposition: Influence of pulse repetition rate " , Solar Energy ,Vol.85 ,pp.1354–1363, (2011) .
54. E. GÜNERI, C. GÜMÜŞa , F. M ANSUR, F. KIRMIZIGÜL , "Studies on properties of sprayed SnO2 thin films as a function of substrate-nozzle distance and substrate temperature",Optoelectronics andadvanced materials – rapid communications Vol. 3, No. 4, p. 383 – 389 , (2009).
55. J. A. R. Márquez. M. B. Rodríguez , C. M. Herrera1 , E. R. Rosas , O. Z.Ange,O.T.Pozos,"Effec of Surface Morphology of ZnO Electrodeposited on Photocatalytic Oxidation of Methylene Blue Dye Part I: Analytical Study" . Int. J. Electrochem. Sci,Vol. 6 ,pp.4059 – 4069 , (2011).
56. T. P. Rao, M.C. Santhosh Kumar , "Physical properties of Ga-doped ZnO thin films by spray pyrolysis" , Journal of Alloys and Compounds .Vol.506,pp. 788–793,(2010) .
57. A. Ivashchenko, and I. Kerner, I.Physical "Approaches to Improvement of Semiconsuctor gas .Sensors Based on SnO2 ",Thin Films –Moldavian J.Phys . Sci, Vol.2,No.1, (2003).
58. Xe . Y, Ye . R. and Lin. H, " Synthesis of silver Nanoparticles in Reverse Micelles Stabilized by Natural Biosurfactant ", Coll . and .Surf

.Colloids and Surfaces A: Physicochemical and Engineering Aspects , Vol. 279 , pp. 175-178, (2006).

59. LC . Nehru, V. Swaminathan , C. Sanjeeviraja , “Photoluminescence Studies on Nanocrystal line Tin Oxide Powder for Optoelectronic Devices”, American Journal of Materials Science ,Vol. 2, No.2,pp.6-10,(2012).
60. J. Gubicza , NQ . Chinh , JL . Labar, Z .Hegedus, P. Szommer, G.Tichy, TG . Langdon. “ Delayed micro structural recovery in silver processed by equal-channel angular pressing ”. J.Mater.Sci, Vol. 43 ,No.16,pp. 5672-5676,(2008).
61. MA . M. Khan, S.Kumar, M . Ahamed, SA .Alrokayan , MS .Alsalhi , “Structural and thermal studies of silver nanoparticles and electrical transport study of their thin films ”. Nanoscale.Res ,Vol. 6,No. 434,pp. 1-8 ,(2011).
62. YPV. Subbaiah , P .Prathap , KTR . Reddy, “Structural electrical and optical properties of ZnS films deposited by close-spaced evaporation ”. Appl.Surf.Sci, Vol.253,No.5,pp. 2409-2415, (2006).
63. S .Velumani , “ X . Mathew, PJ .Sebastian, SaK . Narayandass, D .Mangalaraj, Structural and optical properties of hot wall deposited CdSe thin films”. Solar Energy Materials & Solar cells, Vol.76,No.3,pp. 347-358, (2003).
64. J.Chen , Li .Yelling , Y .Wang , J .Yun , Cao D. “ Preparation and characterization of zinc sulfide nanoparticles under high-gravity environment”, Mat. Res. Bull, Vol . 39,No. 2,pp. 185-194, (2004).
65. J .Zhang , X .Xiao , J .Nan , “ Hydrothermal–hydrolysis synthesis and photocatalytic properties of nano TiO2 with an adjustable crystalline size” , J. Hazardous Mat. Vol .176,pp. 617- 622,(2010).

66. P. Jo-Yong , L .Yun-Jo, J .Ki-Won, JY .Dae , “Chemical Synthesis and Characterization of Highly Oil Dispersed MgO Nanoparticles ”, J. Ind .Eng.Chem, Vol .12,No, 6,pp.882-887,(2006).
67. K.S. Upadhyaya and R.K. Singh, “Shell model lattice dynamics of transition metal-oxides” , J. Phys . Chem .Sol, Vol. 35,No. 1175 ,(1974).
68. J.I. Langford, R.Delhez , Th . H .dekeileijser, E . J .MiHemeijer , “profile analysis for microcrystalline properties by the Fourier and other methods” .Aust. j.phys ,Vol.41,pp.173-187, (1988) .
69. E.J. Mittemeijer and U. Welzel, “The state of the art of the diffraction analysis of crystallite size and lattice strain ”, Z. Kristallogr. Vol .223, pp 552–560, (2008).
70. H. Lin , C.P. Huang . W. Li ,C. Ni , S. I. Shah ,Yao-H. Tseng , “Size dependency of nano crystalline TiO2 on its optical property and photocatalytic reactivity exemplified by 2-chlorophenol ”, Applied Catalysis B: Environmental ,Vol .68 ,pp.1–11,(2006) .
71. G.Shabbir , A. H.Qureshi, K.Saeed ,“ Nano-crystal line $LaFeO_3$ powder synthesized by the citrate – gel method” , Materials letters ,Vol .60,pp.3706 – 3709 ,(2006).

الخلاصة

تم في هذة الدراسة استخدام طريقة فورير لتحليل نمط حيود الاشعة السينية لاوكسيد المنغنيزللقمم (111) ،(200) ،(220)، (311) و(222) ثم تم حساب حجم البلورات لكل قمة. واستخدمت طريقة فورير ايضا لغرض حساب معدل مربع انفعال الشبيكة وكانت النتائج كالاتي حيث حجم البلورات يساوي٦٤٣٥٢.٧ نانومتر و معدل مربع انفعال الشبيكة يساوي ٠,٣٥٦٦ × $١٠^{-٤}$ ولتحديد دقة نتائج هذه الطريقة تم استخدام طرق تحليل اخرى، مثل طريقة ديباي شيرروطريقة وليمسون- هال للتحليل وطريقة ديباي شيررالمعدلة لحساب حجم البلورات وتم تطويرطريقة ديباي شيررلاجل حساب الانفعال واستخدامه في المقارنة . تم مقارنة قيمة حجم الجسيم والانفعال لهذه الطرق الاربعة مع قيمة حجم الجسيم ومعدل مربع الانفعال لطريقة فورير . وتم تطوير طريقة فورير لحساب متغيرات مهمة اخرى في التركيب البلوري ، مثل الانفعال والذي قيمته تساوي. ٧,٤٨٢٨ × $١٠^{-٣}$ بدلا من معدل مربع الانفعال وكثافة طاقة الانفعال والتي قيمتها تساوي ٢٧٩٩٦٤,٧(داين/$سم^{٢}$)والاجهاد والذي قيمته تساوي ٧,٤٨٢٨× $١٠^{٨}$ (داين/$سم^{٢}$) وقد تم استخدام النتائج التي تم الحصول عليها من طريقة فورير لاجل حساب معلمات اخرى لشبيكة اوكسيد المنغنيزلكل قمة من قمم حيود الاشعة السينية مثل معامل البنية البلورية ومعدل قيمته [illegible] والانفعال الدقيق ومعدل قيمته تساو ٤,٤٧× $١٠^{-٣}$ وكثافة الانخلاع ومعدل قيمتها يساوي ٣٧,٣ × $١٠^{١٥}$ (خط . $م^{٢}$) والمساحة السطحية النوعية ومعدل قيمتها يساوي ١٩,٥٨٤٣٢ × $١٠^{٤}$ ($متر^{٢}$/غم). وكذلك تم اجراء مقارنة بين قيم معدل مربع الانفعال والانفعال الظاهري .

جمهورية العراق
وزارة التعليم العالي والبحث العلمي
جامعة بغداد
كلية التربية للعلوم الصرفة - أبن الهيثم

دراسة حجم الجسيمة وانفعال الشبيكه لطور اوكسيد المنغنيز النانوي بواسطة تحليل فورير لحيود الاشعة السينية

رسالة مقدمة إلى

مجلس كلية التربية للعلوم الصرفة – ابن الهيثم – جامعة بغداد كجزء من متطلبات نيل درجة ماجستير علوم في الفيزياء

من قبل
سراب سعدي جحيل

بكلوريوس-(٢٠٠٠)

بأشراف
أ. د. خالد هلال حربي

١٤٣٩هـ **٢٠١٨ م**